AR-008-381

DSTO-TR-0489

Effect of the Leading-Edge Extension (LEX) Fence on the Vortex Structure over the F/A-18

D.H. Thompson

APPROVED FOR PUBLIC RELEASE

19970429 163

DEPARTMENT OF DEFENCE
DEFENCE SCIENCE AND TECHNOLOGY ORGANISATION

Effect of the Leading-Edge Extension (LEX) Fence on the Vortex Structure over the F/A-18

D. H. Thompson

Air Operations Division
Aeronautical and Maritime Research Laboratory

DSTO-TR-0489

ABSTRACT

The effects of the Leading Edge Extension (LEX) fence on the vortex structure over the F/A-18 at moderate to high angles of attack were studied using a 1/9 scale wind tunnel model and a 1/48 scale water tunnel model. Measurements at the tip of one of the vertical fins of the wind tunnel model confirmed that the fence reduced fin vibration caused by vortex breakdown. Flow visualisation in the water tunnel and in the wind tunnel showed that the fence caused the formation of a second LEX vortex, of the same sense as the main LEX vortex, but originating on the LEX leading edge outboard of the fence. Visualisation of the surface flow around the fence showed in detail how the fence caused the second LEX vortex. The effects on vortex breakdown and fin vibration of the interaction between the main and second LEX vortices are discussed.

RELEASE LIMITATION

Approved for public release

DEPARTMENT OF DEFENCE

DEFENCE SCIENCE AND TECHNOLOGY ORGANISATION

Published by

DSTO Aeronautical and Maritime Research Laboratory
PO Box 4331
Melbourne Victoria 3001

Telephone: (03) 9626 8111
Fax: (03) 9626 8999

AR No. AR-008-381
February 1997

Effect of the Leading-Edge Extension (LEX) Fence on the Vortex Structure over the F/A-18

Executive Summary

The high performance of the F/A-18 fighter in air combat manoeuvres is due in large part to its aerodynamic shape, and in particular, to the effect of the sharp, highly-sweptback leading edge extension (LEX) that extends forward from each wing root. At angles of attack typical in air combat manoeuvres, each LEX generates a large vortex above the aircraft. The lifting forces on the F/A-18 due to the LEX vortices give the aircraft its manoeuvring capability.

The manoeuvrability of the F/A-18 does not come without penalty, however. The centreline core of the LEX vortex can undergo the phenomenon of vortex bursting or vortex breakdown. This occurs when smooth, steady airflow along the vortex core suddenly breaks down and becomes disturbed and unsteady. The core also expands considerably in diameter. Under air combat manoeuvring conditions the unsteady flow downstream of the vortex burst position impacts on the fins and tailplane of the aircraft, causing high dynamic loads on these surfaces. Severe structural vibration results, with consequent detrimental effects on the fatigue life of the aircraft structure.

To alleviate the vibration problem the aircraft manufacturer developed the 'LEX fence'. This is a flat trapezoidal plate standing perpendicular to the LEX upper surface and aligned parallel to the aircraft's longitudinal axis. The interference between the fence and the flow beneath the LEX vortex causes a reduction in the dynamic loads applied to the tail, with a consequent reduction in tail vibration and improvement in fatigue life.

The LEX fence was developed using a cut and try process of wind tunnel and flight testing. The aerodynamic mechanism by which the fence achieved its favourable effect was not known. The purpose of the work described in this report was to develop an understanding of the details of the aerodynamic interaction between the fence and the LEX vortex. This understanding will add to DSTO's existing body of knowledge of the aerodynamic characteristics of the F/A-18, will assist in dealing with any future problems that may arise involving the fence, and will assist the International Follow On Test Program (IFOSTP) of fatigue tests on the F/A-18 rear fuselage. It will also assist in the assessment of possible alternatives to the LEX fence should this ever become necessary.

The approach to the problem was to use flow visualisation techniques in a water tunnel and in a wind tunnel to examine the detailed behaviour of the flow in the vicinity of the LEX fence. The vortex flow patterns over the F/A-18 are complex and flow visualisation provides a powerful tool to assist in the understanding of such patterns. In addition, measurements were made of the pressures acting on the aircraft fins and of the accelerations of the fin tips.

The results show that the LEX fence achieves its effect by triggering the formation of a sequence of additional vortices that result in the favourable modification of the vortex breakdown flow. The flow around the fence itself leads to the formation of a vortex originating from a point on the LEX upper surface just outboard of the fence. This vortex in turn modifies the flow around the nearby LEX leading edge and causes the formation of yet another vortex, in this case originating from a point on the LEX leading edge outboard of the fence. This last vortex trails downstream over the LEX and as it does so it intertwines and interacts with the main LEX vortex. It is this interaction that modifies the LEX vortex breakdown process and reduces the dynamic loads on the aircraft fins.

The outcome of this study has been a more detailed knowledge of the flow around the F/A-18 under air combat manoeuvring conditions. In particular, the conditions leading to severe fin vibration, and the way in which these conditions are modified by the LEX fence, are better understood. This understanding will assist in the development of fin loading programs for structural testing, and may be of assistance in the future, should any problems arise with the fence itself. In addition, a detailed knowledge of the fence effect will be useful should it become necessary to seek alternatives to the fence for reducing fin vibration.

Author

D. H. Thompson
Air Operations Division

David completed his Bachelor of Science in Aeronautical Engineering at Queens University, Belfast, in 1965. He completed his PhD at the same university in 1968 and joined Aerodynamics Division of the Aeronautical Research Laboratories in 1969. His main research interests are in experimental subsonic aerodynamics, particularly in the use of flow visualisation techniques in wind and water tunnels to study vortex flows around combat aircraft.

Contents

1. INTRODUCTION

At moderate to high angles of attack, the flowfield above each side of the F/A-18 is dominated by a vortex generated by a highly-swept sharp-edged leading-edge extension (LEX) ahead of each wing root[1]. The pressure field due to each vortex contributes substantially to the lift on the aircraft and confers good manoeuvrability at angles of attack up to about 40°. The vortex also helps maintain attached flow over the outboard wing panel at high angles of attack.

The vertical fins of the F/A-18 are positioned on the aircraft to take advantage of the energetic flow in the LEX vortices and so provide adequate lateral stability and control at high angles of attack. However, breakdown in the vortex cores produces flow unsteadiness that causes vibration of the vertical fins over a range of angles of attack. The horizontal stabilisers may vibrate also, although over a different angle of attack range.

The manufacturers of the F/A-18 alleviated the fin vibration problem by developing the 'LEX fence'. This device is a trapezium-shaped flat plate aligned in a streamwise direction and fixed normal to the LEX upper surface. It is positioned at about the LEX semi-span, at a station just ahead of the junction between the wing and LEX leading edges.

The fences reduce mean velocities and flow angularities in the fin region[2], and reduce fin vibration levels[3,4,5]. For example, in wind tunnel tests, Shah et al[4] measured a reduction in fin leading-edge acceleration of more than 50% when the fence was fitted, and a 20% reduction in the dynamic contribution to the fin root bending moment. Lee et al[3] report a reduction in fin tip acceleration of about 20% with the fence fitted.

The fence has only a small effect on the static longitudinal characteristics of the aircraft, causing little or no loss in maximum lift[2,4], and little increase in drag[2]. The fence does cause a slight nose-down pitching moment increment[2,3,4]. Lee et al[3] report reductions in the magnitude of unsteady variations in lift and pitching moment.

The effect of the fence on the lateral / directional characteristics of the aircraft is less clear. Erickson[2] found little change in these characteristics, but Shah et al[4] report substantial increases in directional stability at angles of attack in the range 15°-30°. These variations may be due to test model differences, as measurement of directional characteristics of this type of aircraft at high angles of attack can be sensitive to small changes in nose geometry.

The fitting of the fence may have non-aerodynamic effects on the aircraft. For example, the addition of a relatively large plate-like projection to the LEX surface is likely to have an unfavourable effect on the radar reflection characteristics of the aircraft, particularly when illuminated from the side.

The fence was developed by a cut-and-try process, with no detailed study of how it worked. Wind tunnel tests[2,3,5,6] and water tunnel tests[7] have provided some details of the flow mechanisms involved. The work reported here provides additional details, using flow visualisation techniques in a water tunnel and in a wind tunnel. The knowledge gained will assist in the design of possible fence modifications, or of possible alternatives to the fence.

2. EXPERIMENTAL PROGRAM

2.1 Water tunnel tests

2.1.1 Test facility

The AMRL water tunnel (Fig. 1) is an Eidetics Model 1520 horizontal-flow tunnel which is operated with a free water surface in the test section. The test section is 380 mm wide, 510 mm deep, and 1.52 m long. The model under test is mounted inverted on a sting which is connected by a C-strut to a turntable. Remotely-controlled direct-current motors move the C-strut and turntable to position the model in pitch and yaw, and digital meters display pitch and yaw angle on the tunnel control panel. The turntable is carried on a rectangular metal plate that is pivoted about its downstream edge and rests on top of the test section. The model support system can be rotated about the pivot to raise the model from the water.

2.1.2 Water tunnel model

The model was based on a 1/48 scale plastic hobby kit of the F/A-18 (Fig. 2). The kit was modified to improve the accuracy of its external representation of the full-scale aircraft. Plastic tubes entering the model interior under the rear fuselage supplied dye to ports positioned at various points on the surface of the model. An internal duct led from each engine inlet to the corresponding exhaust nozzle. A length of brass tube cemented into each nozzle was connected through a valve and flow meter to a suction pump, thus allowing simulation of the flow through each engine inlet. The brass exhaust tubes, clamped in a suitable fitting, also served to mount the model on the sting of the model support system.

Simple bent-metal brackets, attached to the wing and flap undersurfaces with double-sided adhesive tape, supported the wing leading-edge flaps (LEF) and trailing-edge flaps (TEF) at various deflection settings. A small set-screw in the fuselage locked each horizontal tail surface on its spanwise mounting spindle at any desired deflection angle.

Each LEX fence (Fig. 3) was made from thin brass sheet. A small flange along the lower edge allowed the fence to be attached to the LEX upper surface with double-sided adhesive tape.

2.1.3 Flow visualisation techniques

One of the flow visualisation techniques used in the tests involved the injection of coloured dyes into the flow through ports in the model surface. A dye port was located on each side of the fuselage, just beneath the apex at the forward end of each LEX. Another dye port was located on each LEX upper surface at about 50% of the LEX chord and 50% of the LEX semispan, and another at a similar position on each LEX lower surface. Dye containers pressurised by air from a small compressor supplied liquid food dyes or fluorescein sodium dye to the ports. A needle valve in each dye line controlled the flow rate.

Another flow visualisation technique used in the tests involved the electrolytic generation of minute hydrogen gas bubbles to act as flow tracers. The cathode of the electrolytic circuit was a narrow strip of aluminium foil cemented beneath the leading edge of the LEX. The anode was another foil strip cemented to the model surface nearby. The cathode strip generated a continuous sheet of bubbles which separated from the leading edge and passed into the vortex system above the LEX.

Three 150 W tungsten spotlamps mounted in front of and/or beneath the test section provided general illumination of the model and dye patterns. Two of these spotlamps mounted beneath the test section provided illumination of the hydrogen bubbles.

Making visible the flow patterns in cross-flow planes in a vortical flow can provide considerable insight into the structure of the flow. This approach is particularly effective when used with hydrogen bubbles shed from the LEX leading edge and illuminated using a laser light sheet. In this case, a Lexel Model 65 air-cooled argon ion laser, positioned beneath the test section and producing about 35 mW of power at a wavelength of 488 nm, acted as a light source. A glass rod expanded the laser output beam into a fan-shaped sheet, and a small scanning mirror reflected the sheet up into the test section. Driving the scanning mirror to preselected angles placed the light sheet at different positions on the model. Alternatively, driving the mirror with a triangular or sawtooth waveform swept the light sheet repeatedly through the flow volume of interest. A camera positioned at the downstream window in the tunnel diffuser recorded the bubble patterns in the light sheet.

Flow tracers originating at a number of closely-spaced points on the model surface can help in the detailed examination of the flow over some parts of the model. Usually, fitting dye ports at the required surface distribution is not practical, particularly with small models such as the one used for these tests. Also, the optimum positioning of each port requires some prior knowledge of the flow pattern.

Development of a technique based on the well-known oil dot surface flow visualisation method[8] overcame these problems. The technique is best suited for use in a water tunnel with a free surface in a horizontal test section, allowing easy model access. To use the technique, the model on its pivoted mounting was raised from the water and dried. Small dots of a dyed paste were applied to the model surface. With the flow velocity and model angle of attack set at the desired values, the model was replaced in the test section. The paste dots acted as dye sources for periods of up to several minutes, depending on the flow pattern and stream velocity.

The paste consisted of ordinary gel toothpaste, well mixed with a small amount of fluorescein sodium dye powder. The toothpaste acted as a convenient form of slow-release binder for the dye. A small syringe, with a length of hypodermic tubing replacing the needle, served as an applicator for the paste. By slowly extruding the paste through the tubing it was possible, with a little practice, to place dots of a reasonably uniform size (< 1mm diameter) as required on the model surface.

The flow patterns produced by the various visualisation techniques were recorded on videotape, using a video camera and a video cassette recorder, or on film, using a single-lens-reflex film camera. An image processing system installed in a personal computer stored and processed images taken directly from the video camera or from the videotape. Software was available to make measurements from the stored images.

2.1.4 Experimental procedure

While dye was injected into each vortex core through a port beneath each LEX apex, plan views and side views of the pattern of vortex flow and vortex breakdown above the model were recorded. From stored images, vortex breakdown position and model angle of attack were measured against a reference grid. Measurements were made over a range of angles of attack from 12° to 45°, with and without the LEX fence fitted.

At selected angles of attack, details of the flow on and above the LEX upper surface were made visible using dye injected through ports on the LEX upper surface and beneath the LEX leading edge. The paste-dot flow visualisation technique provided details of the flow on and near the surface of the LEX in the vicinity of the fence. The hydrogen bubble technique, in conjunction with the scanning laser light sheet provided cross-sectional flow patterns of the vortex system at and downstream of the fence.

The freestream velocity for most of the tests was 80 mm/s, corresponding to a Reynolds number of 5120, based on wing mean aerodynamic chord.

2.2 Wind tunnel tests

2.2.1 Test facility

The ARL 2.7m by 2.1m low speed wind tunnel is a closed-return-circuit tunnel with a closed test section. A sting-column rig supports models in the test section.

2.2.2 Wind tunnel model

The wings, stabilators, fins and fuselage shell of the 1/9th scale wind tunnel model[5] of the F/A-18 were made mostly of carbon fibre. High tensile aluminium spars reinforced the wings and tail surfaces where required. High tensile aluminium also formed the structural sub-frame and load attachment points of the model.

With the leading-edge flaps deflected to 34° and the trailing-edge flaps undeflected, the wing configuration corresponded to that required for flight at angles of attack greater than 25.6° and Mach numbers less than 0.6.

The tests did not include force or moment measurements, so the model was mounted on a dummy strain gauge balance on the pitch/roll sting-column rig. The model end of the sting consisted of two parallel tubular members passing through the engine exhaust nozzles. Venting of the model internal volume through the hollow sting members allowed flow-through engine inlet operation.

2.2.3 Instrumentation

A pressure transducer and an accelerometer were located on the outboard side of the port fin tip, as shown in Figure 4. Two surface-mounted pressure transducers were located on the rear upper surface of the port wing, just outboard of the wing root.

All transducer output signals were recorded and analysed using a Wavetek 804A Fast Fourier Transform (FFT) Analyser. Calibration of the transducers against a reference Digiquartz pressure transducer of known accuracy showed that the transducer characteristics were within 1% of the manufacturer's calibration certificate values. All data reduction during the tests used these certificate values. The FFT Analyser displayed the processed results as graphs of power spectral density (PSD) versus frequency.

2.2.4 Flow visualisation techniques

Smoke injected into the LEX vortex from a probe positioned with its tip just below the LEX apex marked the vortex core and the vortex breakdown. Movement of the smoke probe along the LEX leading edge marked other parts of the LEX vortex system as required. A light box and slit, mounted on the roof of the tunnel test section, provided illumination in the form of a light sheet with its plane oriented along the axis of the vortex. The smoke patterns were recorded on videotape.

The laser and optical system used for the water tunnel tests also provided a scanning light sheet for visualisation of crossflow sections of the smoke patterns in the LEX vortex system in the wind tunnel.

Surface flow patterns were visualised using a variation of the oil-dot technique[8]. A sheet of self-adhesive vinyl material (trade name "Contact") was applied to the model surface in the area of interest. Careful stretching and trimming of the vinyl gave a smooth surface matched to the model curvature and edges. A length of hypodermic tube (0.5 mm internal diameter) was used to apply "Zyglo" dye to the surface of the vinyl in the form of small dots, typically 1 mm in diameter. "Zyglo" is a yellow-green fluorescent penetrant dye used for crack detection in materials science.

As quickly as possible after the application of the dots, the wind tunnel was started and brought up to speed. Under the action of viscous forces dye from the dots formed into streaks on the surface, indicating the direction of the local surface flow. "Blacklight" fluorescent tubes mounted around the test section illuminated the dye patterns with ultra-violet light. When the flow patterns had stabilised, the tunnel was shut down and the flow patterns were photographed in situ on the model.

The vinyl served several purposes. It protected the model surface from staining by the dye and it provided an appropriate background colour for the dye traces. Tests showed that white "Contact" gave the best results, fluorescing blue and providing an excellent background to the yellow-green dye traces. With care, the vinyl could be removed from the model surface, complete with the flow pattern, and mounted on card for further photography and storage.

Unless care was exercised when applying the vinyl, the material could be pressed into the small gaps around access panels on the model surface. Dye moving across the surface from the applied dots and encountering these indentations tended to travel along the line of the panel joint, giving misleading indications of the surface flow direction. Some examples of this problem will be discussed below.

2.2.5 Experimental procedure

The tunnel airspeed for the smoke flow visualisation tests was 5 m/s, corresponding to a Reynolds number based on mean aerodynamic chord (R_{mac}) of 1.3 x 10^5. With smoke injected into the vortex core, vortex trajectories were recorded for a range of angles of attack from 19° to 30°, with and without the LEX fence in place. A camera located outside the test section recorded side views of the model. Another camera located inside the test section recorded views of the vortex pattern from a position above and behind the model. With smoke injected near the leading-edge of the LEX, vortex cross-sections in the vicinity of the fence were recorded from a camera position behind and slightly below the model.

Fin tip accelerations and pressures, and wing upper surface pressures were recorded and analysed for an airspeed range from 20 to 50 m/s (R_{mac}= 4.2 x 10^5 to 1.3 x 10^6), and an angle of attack range from 19° to 30°, with and without the fence in place.

The surface flow patterns in the region of the fence on the LEX upper surface were recorded with and without the fence in position. The velocity was 50 m/s and the angle of attack ranged from 19° to 30°.

3. RESULTS AND DISCUSSION

3.1 Effect of LEX fence on fin vibration

The design of the fin on the 1/9 scale wind tunnel model made no attempt to represent the stiffness or dynamic structural characteristics of the full-scale fin. However, the frequency of the first bending mode of the model fin was such that this mode was excited by the vortex breakdown flowfield in the wind tunnel tests. Measurements of fin tip accelerations on the wind tunnel model confirmed the effectiveness of the LEX fence in reducing fin vibration levels.

Figures 5 and 6, for angles of attack of 25.4° and 30.5° respectively, show typical effects of the LEX fence on the power spectral density (PSD) levels of the fin tip acceleration and the fin tip and wing upper surface pressures at airspeeds of 30, 40 and 50 m/s. When comparing the plotted results, note that the vertical scales vary, to allow retention of reasonable detail.

The fence reduces the peak PSD levels of the fin tip accelerations and fin tip pressures by factors that vary between two and three over the angle of attack and velocity ranges. The wing upper surface pressure peak PSD levels are reduced by a factor of more than ten. The frequency at which the fin tip and wing upper surface pressure peaks occur increases with airspeed.

These results showing the favourable effect of the fence are in agreement with other published measurements of fin vibration levels, such as those by Lee et al[3], Shah et al[4], and Martin et al[5]. However, these measurements alone give no indication of the mechanism by which the fence achieves its effect.

3.2 Effect of LEX fence on vortex breakdown position

The possibility that the fence might achieve its favourable effect by shifting the vortex breakdown away from the fin was investigated using dye in the water tunnel and smoke in the wind tunnel. The change in the longitudinal position of vortex breakdown with angle of attack, with fence off and fence on, is plotted in Figure 7. There is reasonable agreement between the water tunnel and wind tunnel results. For angles of attack below about 15°, the breakdown is located downstream of the fin leading edge. The breakdown moves upstream with increasing angle of attack, and for angles of attack above about 30°, is located upstream of the fence position. The fitting of the fences has little effect on the longitudinal position of the breakdown.

Additional measurements showed that the fence also had little effect on the lateral position of the vortex breakdown. Thus the beneficial effects of the fence are not due to any significant change in vortex breakdown position relative to the fin.

3.3 Effect of LEX fence on vortex path and breakdown appearance

In water tunnel tests at angles of attack where the fence is upstream of the breakdown, the fence distorts the dye filament marking the vortex core upstream of the breakdown. This distortion is also apparent in wind tunnel tests with smoke marking the vortex core.

Figure 8 shows comparative side and plan views of the model, with the fence off and the fence on, at various angles of attack in the water tunnel. The apparent double images of parts of the vortex core seen in some of the plan views are shadows of the dye filaments on the model surface.

At an angle of attack of 19.5° (Fig. 8(a) and (b)), the fence causes a slight helical deformation in the vortex core, seen more clearly in the plan view (Fig. 8(b)). The core is deflected upward and inboard, then downward and outboard. The breakdown itself is shifted outboard slightly.

The vortex core deformation caused by the fence is less apparent at an angle of attack of 25.4° (Fig. 8(c) and (d)), than at the lower angle of attack of 19.5°. At an angle of attack of 30.5° (Fig. 8(e) and (f)), vortex breakdown occurs in the vicinity of the fence position, and the fence does not affect the shape of the vortex core upstream of the breakdown.

For angles of attack up to about 27°, breakdown occurs downstream of the fence position, and the addition of the fence alters the appearance of the breakdown. With the fence off, a sudden expansion of the core dye filament clearly defines the breakdown. With the fence on, the breakdown appears less distinct, with a gradual thickening of the core dye filament upstream of the breakdown proper. This change in appearance can be seen in Figure 8(a) for an angle of attack of 19.5° and in Figure 8(c) for an angle of attack of 25.4°.

Similar changes in vortex core shape and breakdown appearance were observed in the wind tunnel tests. The video images in Figure 9 show the LEX vortex cores, visualised using smoke, with and without the fence, for three angles of attack. Figures 9(a) - (d), for angles of attack of 19.5° and 25.4°, show that with no fence fitted, the position and appearance of the vortex breakdown match those seen in the water tunnel, with a straight core filament upstream of a clearly-defined breakdown occurring ahead of the fin leading edge.

The fence causes a helical deformation of the vortex core. The deformation appears more pronounced than in the water tunnel. As in the water tunnel tests, the fence alters the appearance of the vortex breakdown, with a clearly-defined sudden expansion being replaced by a more gradual thickening of the core.

At an angle of attack of 30.5° (Fig. 9(e) and (f)), the breakdown occurs close to the fence position. As in the water tunnel tests, the fence does not affect the core shape upstream of the breakdown.

In summary, when the vortex breakdown is downstream of the fence, the fence causes a helical deformation of the vortex core upstream of the breakdown. The fence also changes the appearance of the breakdown itself from a clearly defined sudden expansion of the core to a more gradual expansion or thickening of the core. When the vortex breakdown is upstream of the fence, the core trajectory and the appearance of the breakdown remain unaffected by the fence. Nevertheless, the fence is still effective in reducing the level of fin vibration. Thus the mechanism by which the fence operates still functions, even when the fence is immersed in the flowfield of the broken-down vortex.

3.4 Interaction between LEX fence and LEX vortex flow field

To find out more about the interaction between the fence and the LEX vortex, experiments were performed to visualise the LEX vortex flowfield outside the core region.

In the water tunnel, the hydrogen bubble technique with a laser light sheet provided more information on the behaviour of the flow separating from the LEX leading edge in the vicinity of the fence. As an example, Figure 10 shows successive sections through the hydrogen bubble pattern as the laser beam moves downstream past the fence location. Well upstream of the fence, the vortex cross section is typical of that above a wing with a highly-swept leading edge. The layer of fluid separating from the leading edge rolls up smoothly into a spiral vortex above the LEX and inboard of the leading edge. Further downstream, in the vicinity of the fence, a kink appears in the separated layer. The kink develops into a second vortex, rotating in the same sense as the main LEX vortex. The mutual interaction between the vortices causes the second LEX vortex to move upwards and inboard over the main LEX vortex, then downwards on the inboard side of the main LEX vortex. The interaction also distorts the main LEX vortex core into the helical shape previously described and discussed. Further downstream, the two vortices merge.

Figure 10(b) shows a side view of the fence region of the model with the hydrogen bubbles separating from the leading edge and marking the main LEX vortex and the second LEX vortex. The path of the second LEX vortex climbing away from the surface and moving inboard above the main LEX vortex can be seen.

Similar effects were observed using the laser with smoke in the wind tunnel. The photographs in Figure 11 show a cross-section through the smoke in the LEX vortex system just downstream of the fence trailing edge. The camera position was downstream and inboard of the light sheet position. The upper image is taken directly from the videotape while the lower image has been processed digitally to enhance the edges of the vortex cross-sections.

The uppermost vortex cross-section is that of the main LEX vortex. Below it and slightly outboard is the cross-section through the second LEX vortex, which is in the process of lifting upwards away from the LEX leading-edge.

The second LEX vortex was observed by Martin et al[5] in earlier wind tunnel tests of the model used for the work described in this report. Erickson[2], using a 0.06-scale model in wind tunnel tests at the David Taylor Research Center, also observed the occurrence of a second LEX vortex caused by the presence of the fence.

At angles of attack of 30° or more, when vortex breakdown occurred upstream of the fence, visualisation in water and in air showed that the second LEX vortex caused by the fence was still present. The unsteady flow conditions within the breakdown region made observation of flow details difficult, but the second LEX vortex still interacted with and distorted the LEX vortex flowfield.

An unusual flow pattern was observed in the water tunnel, for a small angle of attack range with the fences fitted. Dye injected at the LEX apex did not clearly define the vortex breakdown. In the vicinity of the breakdown, the dye filament in the vortex core was deflected off the core axis and spread out into an asymmetric curved sheet, without displaying the core thickening or core axis stagnation characteristic of vortex breakdown. To study this flow pattern in more detail, dye was injected through a hole on the LEX underside at about the same chordwise position as the fence. The dye passed outboard beneath the LEX, upwards around the LEX leading edge and into the second LEX vortex. More dye injected through a hole on the LEX upper surface upstream of the fence passed downstream over the LEX upper surface and into the second LEX vortex.

Figure 12 shows two examples of the flow patterns observed. The principal breakdown actually occurs in the second LEX vortex, as shown in the upper photograph. The deflection and spreading of the main LEX vortex core dye is due to the core deflecting around the breakdown in the second LEX vortex, as shown in the lower photograph in Figure 12. This flow pattern occurred at relatively low flow velocities (about 30 mm/s), and for an angle of attack range of about 17° - 22°. At higher velocities, distinguishing which vortex broke down first was impossible, due to diffusion and mixing of the dye filaments. However, breakdown of the second LEX vortex may be another factor contributing to the complexity of the vortex interactions caused by the fence.

Observations suggest that the LEX fence causes the formation of a second LEX vortex, which originates at the LEX leading edge, outboard of the fence, and rotates in the same sense as the main LEX vortex. The two vortices interact. When the breakdown is aft of the fence, the interaction causes a helical deformation of the main LEX vortex core upstream of the breakdown. When the breakdown is ahead of the fence, the interaction causes a distortion of the brokendown flowfield. The processes by which the fence causes the formation of the second LEX vortex and by which the second LEX vortex reduces the fin vibration require further explanation.

3.5 Details of flow around LEX fence

To determine how the LEX fence causes the formation of the second LEX vortex, the flow behaviour close to the fence was examined in detail. In the water tunnel, the dyed paste dot technique was used to study the flow patterns on and near the fence and the adjacent LEX upper surface. A pattern of paste dots on the LEX upper surface covered an area extending from just upstream of the fence to just downstream of the junction of the LEX and wing leading edges. Figure 13(a) shows a video image of a typical flow pattern outboard of the fence, and Figure 13(b) is a perspective sketch of the flow pattern, based on direct visual observation and study of videotape.

Figure 13(a) shows how dye from upstream and inboard of the fence moves outboard ahead of the fence, curves around the fence and moves downstream. Dye from outboard of the fence leading edge moves downstream, curves inboard towards the fence, turns upstream, and finally lifts away from the surface in a spiral. Dye originating from dots just outboard of the fence trailing edge moves upstream into the region where fluid is spiralling away from the surface. Dye from further outboard of the fence trailing edge moves downstream and outboard.

The most significant flow feature indicated by motion of the dye from the paste dots is the vortex-like structure springing from the LEX surface outboard of the fence. For convenience, this structure will be referred to as the "fence vortex". The fence vortex is centred at about one-third of the fence length from the fence leading edge and, on the starboard side of the aircraft, rotates in a clockwise direction when viewed from above. The axis of the fence vortex is initially almost normal to the LEX surface, subsequently bending over in a downstream direction. Details of the structure become obscure as it merges with the LEX vortex system. The fence vortex induces flow in an upstream direction on the LEX surface just outboard of the fence, and on the outboard surface of the LEX fence itself.

The fence vortex is distinct from the second LEX vortex that interacts with the main LEX vortex downstream of the fence. The fence vortex is of opposite sense to the main LEX vortex and originates at the LEX surface. The second LEX vortex is of the same sense as the main LEX vortex and originates from somewhere on or near the LEX leading edge. Figure 13(b) shows diagrammatically the spatial relationship between these three vortex structures.

In the wind tunnel, the Zyglo dot technique was used to produce surface flow patterns on the upper surface of the starboard LEX in the vicinity of the fence position, with and without the fence fitted. Some typical results are shown in Figure 14. The most significant features of the flow patterns are similar for each of the three angles of attack illustrated (19.5°, 25.4° and 30.5°), and the following comments apply to all these cases. (Note that in Figure 14(a) and (b), the apparent sudden outboard turning and coalescence of several dye lines near the left-hand (downstream) edge of the vinyl is due to dye moving along a panel joint, into which the vinyl surface covering has been pressed. This problem was discussed in Section 2.2.4 above.)

With no fence fitted, the dye pattern on most of the LEX surface is dominated by S-shaped dye lines sweeping outboard and downstream. This is a characteristic pattern produced on a lifting surface at high angles of attack by a vortex originating from a highly-swept leading edge. In this case, the pattern is due to the main LEX vortex, rotating in a counter-clockwise direction when viewed from downstream. The outboard ends of the dye lines coalesce in a separation line. Outboard of the separation line is a zone where no definite vortical flow is apparent. At the outboard edge of this zone is another separation line formed by the coalescence of dye lines moving inboard and downstream. These lines indicate the presence of a secondary vortex that is located further outboard and closer to the LEX surface than the main LEX vortex, and rotates in the opposite direction.

Close to the inboard edge of the LEX, the surface dye traces diverge from a line running parallel to the fuselage side. This divergence indicates the presence of an attachment line on the LEX surface, consistent with the presence of a small vortex in the corner between the LEX upper surface and the fuselage side. This corner vortex rotates in the opposite direction to the main LEX vortex.

Figure 14 shows that the fence causes considerable changes in the surface flow patterns. The patterns are similar to those seen using dyed paste in the water tunnel tests. Figure 15 shows additional views of flow on the LEX surface and on the inboard and outboard surfaces of the fence itself. Figure 16 shows a sketch of a proposed surface flow pattern, based on the photographs of Figures 14 and 15, and additional photographs not shown here. The following discussion refers to several flow features labelled in Figure 16.

The dye patterns show that flow sweeping outboard beneath the main LEX vortex is deflected by the fence. Some surface dye lines pass around the leading edge of the fence, while others are deflected downstream, inboard of the fence. There is an indication, particularly in Figure 14(a), of a possible saddle point (SP1) inboard, and slightly downstream, of the fence leading edge. Other photographs, not shown here, with slightly different dye spot positions, gave stronger indications of the presence of this saddle point.

Dye lines originating just upstream of SP1 pass outboard around the leading edge of the fence, turn downstream, then inboard, and then upstream into a focus (N) on the LEX upper surface, just outboard of the fence. The sense of rotation of the focus is clockwise on the starboard LEX when viewed from above. Upstream of the fence, the two secondary separation lines S1 and S2 are first deflected outboard as they approach the fence leading edge. Then they turn inboard and upstream into the focus N. Dye lines from points just outboard of the fence pass upstream into the focus.

Directly downstream of the focus and outboard of the fence trailing edge, there is evidence of another saddle point (SP2). Outboard of the saddle point, in region A, dye lines sweeping outboard towards the LEX leading edge indicate the presence of the second LEX vortex, rotating in the same sense as the main LEX vortex. The origin of the second LEX vortex lies at the LEX leading edge, outboard of the focus N. The trace of the second LEX vortex is no longer apparent further downstream. This is consistent with the second LEX vortex rising away from the surface and moving inboard above the primary LEX vortex.

On the outboard surface of the fence itself, the dye lines indicate the presence of a node near the trailing edge. Upstream of the node, the dye lines indicate flow in an upstream direction, induced on the fence by the fence vortex originating from the focus N. Close to the upper edge of the fence, the dye line direction has an upward component, and this upward component becomes more dominant towards the fence trailing edge. This change in direction of the dye lines is what would be expected as the fence vortex bends over in a downstream direction.

Inboard of the fence, downstream of the saddle point SP1, the predominant flow direction is downstream. There is some indication of convergence on to a separation line S3, stretching downstream from SP1, with flow directed inboard from the fence base towards the separation line. On the inboard surface of the fence itself, the flow direction is mainly downstream. An upward flow component near the fence upper edge and a downward flow component near the fence base indicate a divergence from an attachment line running along the fence at about one third of its height from the base.

The downward flow near the fence base, together with the flow on the LEX surface directed inboard away from the fence base , indicate the presence of a small vortex in the corner between the fence and the LEX. This vortex is of the opposite sense to the main LEX vortex, and could be interpreted as one part of a necklace vortex system formed by the interaction between the fence and the outward flow beneath the main LEX vortex. The necklace vortex would be expected to pass around the fence leading edge, but it is absorbed by the flow passing into the focus N and is not apparent on the outboard side of the fence.

With the flow structure proposed here, a cross-section of the flow near the fence trailing edge would show the main and second LEX vortices, as identified in Figure 11. The smoke-filled structure just above the fence in Figure 11, slightly below and inboard of the main LEX vortex, can be identified as the fence vortex, with its axis curved over to lie roughly parallel to the LEX surface.

In summary, the fence vortex induces motion in an inboard direction on fluid near the LEX leading edge, outboard of the fence. Locally, fluid flowing over the LEX leading edge experiences a change in effective leading-edge sweepback angle. The change in effective sweep angle causes a splitting of the leading edge vortex sheet and the formation of a new leading-edge vortex. (In this respect, the fence vortex has an aerodynamic effect similar to the kink in the leading edge of a double-delta wing.) The interaction between the new leading-edge vortex and the main LEX vortex leads to the effects on vortex breakdown already discussed.

In wind tunnel tests on a 6% scale model of the F/A-18, Lee and Valerio[6] used the oil dot visualisation technique to study the flow on the fence and on the LEX surface near the fence. Their sketch of the surface flow patterns shows several of the features described in the present report. These include the focus on the LEX surface outboard of the fence, the traces of the second LEX vortex downstream of its origin at the LEX leading edge, and the attachment line on the LEX surface due to the vortex in the corner between the LEX and the fuselage side.

Their sketch also shows a saddle point on the LEX surface inboard of the fence leading edge, and an associated focus. As discussed above, the present tests showed some evidence of the saddle point. There was no evidence of the focus, but this may have been due to the distribution of dye spots in this region.

The saddle point (SP2) outboard of the fence was not observed by Lee and Valerio[6]. Also, their sketch gives no indication of upstream flow on the LEX surface just outboard of the fence.

Lee and Valerio[6] propose a structure for the off-surface flow topology near the downstream end of the fence at an angle of attack of 30°. They suggest that a vortex is shed at the upper edge of the fence. This vortex, rotating in the opposite sense to the main LEX vortex, lies outboard of the fence and has its axis aligned in a streamwise direction. They suggest that because this vortex lies close to the primary vortex sheet separating from the LEX leading edge, it will cause an instability and kink in the primary sheet, as in Figure 10 above, leading to the development of the second LEX vortex.

In the tests described here, the fence vortex springing from the focus (N) on the LEX surface occupies the position of the fence edge vortex proposed by Lee and Valerio[6]. As discussed above, it is considered that a change in local effective sweep angle induced by the fence vortex causes the formation of the second LEX vortex, rather than the sheet instability proposed by Lee and Valerio[6].

Lee and Valerio[6] also suggest the presence of a small vortex located in the outboard corner between the fence and the LEX surface. This vortex was not observed in the present tests.

3.6 Effect of co-rotating vortices on vortex breakdown

In several studies, the position of vortex breakdown over wings with highly-swept leading edges has been shown to be influenced by the interaction between a co-rotating vortex and the main wing vortex. The co-rotating vortex may be due to the presence ahead of the wing of a strake[10], a chined forebody[11], or a canard surface [12,13]. The interaction generally results in a downstream displacement of the vortex breakdown over the wing, relative to the wing-alone case. This effect is probably due to a modification of the axial pressure gradient along the core of the main LEX vortex. Vortex breakdown is sensitive to pressure gradient.

In the case of the F/A-18, the breakdown is not shifted significantly by the fence-induced co-rotating vortex, but the appearance of the breakdown is altered. The fence is effective even when the breakdown occurs upstream of the fence location. Thus, the mechanism by which the fence operates must be different from a simple shift in breakdown position.

The fence reduces the strength of the main LEX vortex by causing a split in the vortex sheet separating from the LEX leading edge. Downstream of the split, vorticity shed by the LEX leading edge no longer increases the strength of the main LEX vortex, but instead feeds into the second LEX vortex. The process is similar to that which occurs over double delta wings, for example, as described by Verhaagen[10] and by Smith[14]. The result is that the vorticity originally concentrated in one vortex is redistributed between two vortices, and this occurs even if the individual vortices have broken down. Only the short length of LEX leading edge between the point of origin of the second vortex and the junction with the wing leading edge is available to feed vorticity into the second vortex. Nevertheless, the redistribution of vorticity in the two-vortex system is sufficient to markedly reduce the unsteady loads applied to the vertical fins.

The redistribution of vorticity has been demonstrated experimentally. Lee et al[3] report on measurements made using a pressure sensor rake behind the fin of an F/A-18 wind tunnel model. Their results show that, at an angle of attack of 30°, the effect of the fence was to stretch the pressure coefficient contours laterally and to reduce the peak velocities in the vortex flowfield.

Martin et al[5] traversed a static pressure probe through a vortex with and without the fence fitted. They detected high PSD pressure levels at the upper and lower edges of the vortex flowfield without the fence. These high PSD levels were reduced by a factor of ten when the fence was fitted. In addition, PSD pressure levels on the vortex centre line were reduced by a factor of two.

Erickson[2] reports on McDonnell Douglas tests on an earlier version of the fence which showed reduced velocity magnitudes and flow angularities in the vicinity of the fin.

4. CONCLUSIONS

The effects of the LEX fence on the vortex flow over the F/A-18 have been studied using flow visualisation tests on a 1/48-scale water tunnel model and on a 1/9-scale wind tunnel model. In addition, pressures and accelerations were measured at the tip of one of the vertical fins of the wind tunnel model. These measurements confirmed that the fence considerably reduced fin vibration levels.

The flow visualisation results show that the LEX fence has only a small effect on longitudinal and lateral position of the LEX vortex breakdown.

The favourable effect of the fence on the fin vibration is due to a second LEX vortex caused by the fitting of the fence. The second LEX vortex is of the same sense as the main LEX vortex and is triggered by another vortex originating from the LEX upper surface just outboard of the fence. This fence vortex deflects the main LEX flow pattern in an inboard direction, disrupting the leading-edge vortex sheet that feeds the primary LEX vortex. Where this disruption occurs, the second leading-edge vortex begins to form.

The fence and its associated fence vortex thus produces an aerodynamic effect similar to that of the kink in the leading-edge of a double-delta wing.

The second LEX vortex interacts favourably with the primary LEX vortex, changing the characteristics of the flow by redistributing vorticity within the breakdown flowfield. These changes reduce markedly the unsteady pressure loadings on the fin, with a consequent reduction in fin vibration levels.

ACKNOWLEDGEMENTS

The author would like to acknowledge the helpful discussions he had with Dr Richard Kelso during the course of this work, and also the expert assistance of the staff of the AMRL Low-Speed Wind Tunnel in carrying out the wind tunnel tests.

REFERENCES

1. Erickson, G. E. (1982) *Water tunnel flow visualisation and wind tunnel data analysis of the F/A-18*, NASA CR-165859

2. Erickson, G. E. (1991) *Wind tunnel investigation of vortex flows on F/A-18 configuration at subsonic through transonic speeds*, NASA TP-3111

3. Lee, B. H. K., Brown, D., Zgela, M. & Poirel, D. (1990) Wind tunnel investigation and flight tests of tail buffet on the CF-18 aircraft, *AGARD Specialists' Meeting on Aircraft Loads due to Flow Separation*, Sorrento, Italy, 1-6 April, 1990, Paper 1.

4. Shah, G. H., Grafton, S. B., Guynn, M. D., Brandon, J. M., Dansberry, B. E. & Patel, S.R. (1990) Effect of vortex flow characteristics on tail buffet and high angle of attack aerodynamics of a twin-tail fighter configuration, *High Angle of Attack Technology Conference*, NASA Langley Research Center, 30 October - 1 November 1990

5. Martin, C. A., Glaister, M. K., MacLaren, L. D., Meyn, L. A. & Ross, J. (1991) *F/A-18 1/9th scale model tail buffet measurements*, Aeronautical Research Laboratory, Flight Mechanics Report 188

6. Lee, B. H. K. & Valerio, N. R. (1994) Vortical flow structure near the F/A-18 LEX at high incidence, *AIAA Journal of Aircraft*, 31, 1221-1223

7. Thompson, D. H. (1990) *Water tunnel flow visualisation of vortex breakdown over the F/A-18*, Aeronautical Research Laboratory, Flight Mechanics Report 179

8. Meyer, R. F. (1996) *A note on a technique of surface flow visualisation*, National Research Council of Canada, Aeronautical Report LR-457

9. Thompson, D. H. (1985) *A visualisation study of the vortex flow around double-delta wings*, Aeronautical Research Laboratory, Aerodynamics Report 165

10. Verhaagen, N. G. (1983) *An experimental investigation of the vortex flow over delta and double-delta wings at low speed*, Delft University of Technology, Dept. of Aerospace Engineering, Report LR-372

11. Hall, R. M. (1987) Influence of forebody cross-sectional shape on wing vortex-burst location, *AIAA Journal of Aircraft*, 24, 645-652

12. Er-El, J. & Seginer, A. (1985) Vortex trajectories and breakdown on wing-canard configurations, *AIAA Journal of Aircraft*, 22, 641-648

13. Thompson, D. H. (1992) *Flow visualisation in water of vortex flow over sharp-edged canard configurations*, Aeronautical Research Laboratory, Flight Mechanics Report 189

14. Smith, J. H. B. (1984) Three-dimensional modelling of vortex flows in aerodynamics, *Aeronautical Journal*, 88, 101-116

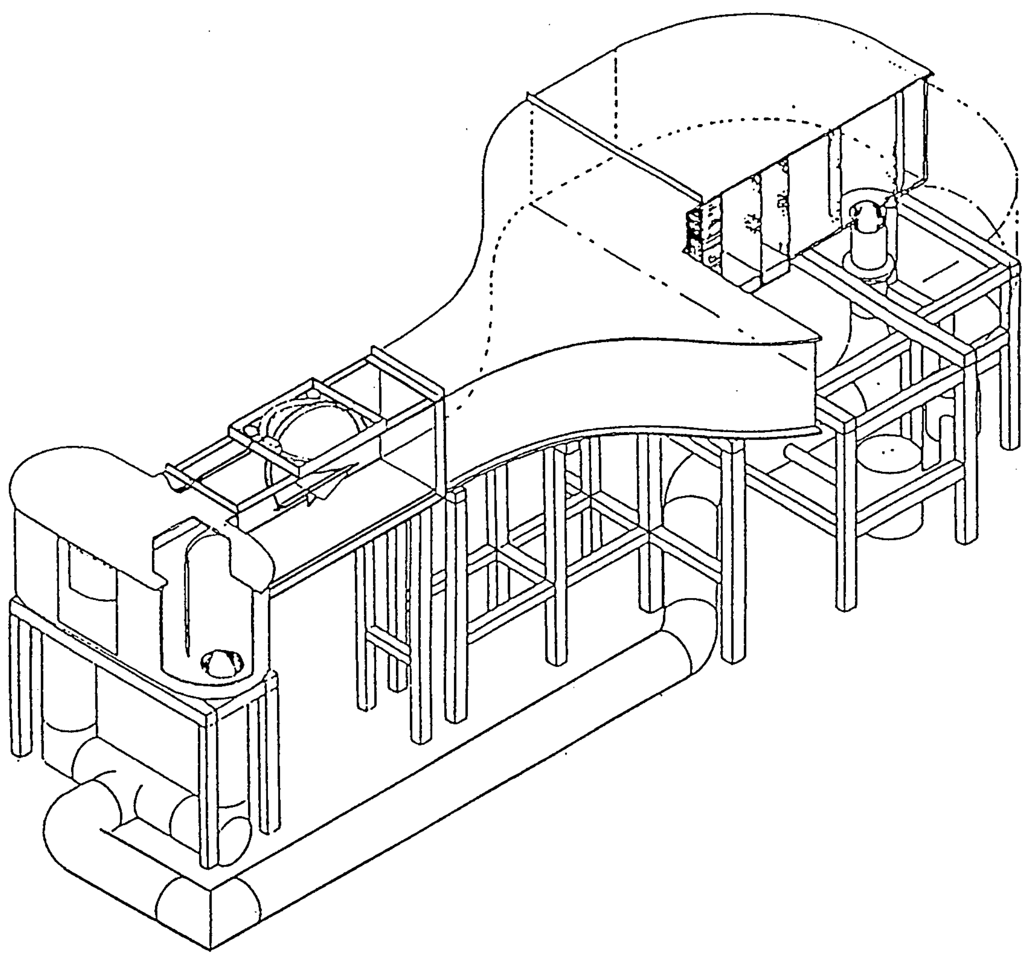

Figure 1. AMRL water tunnel

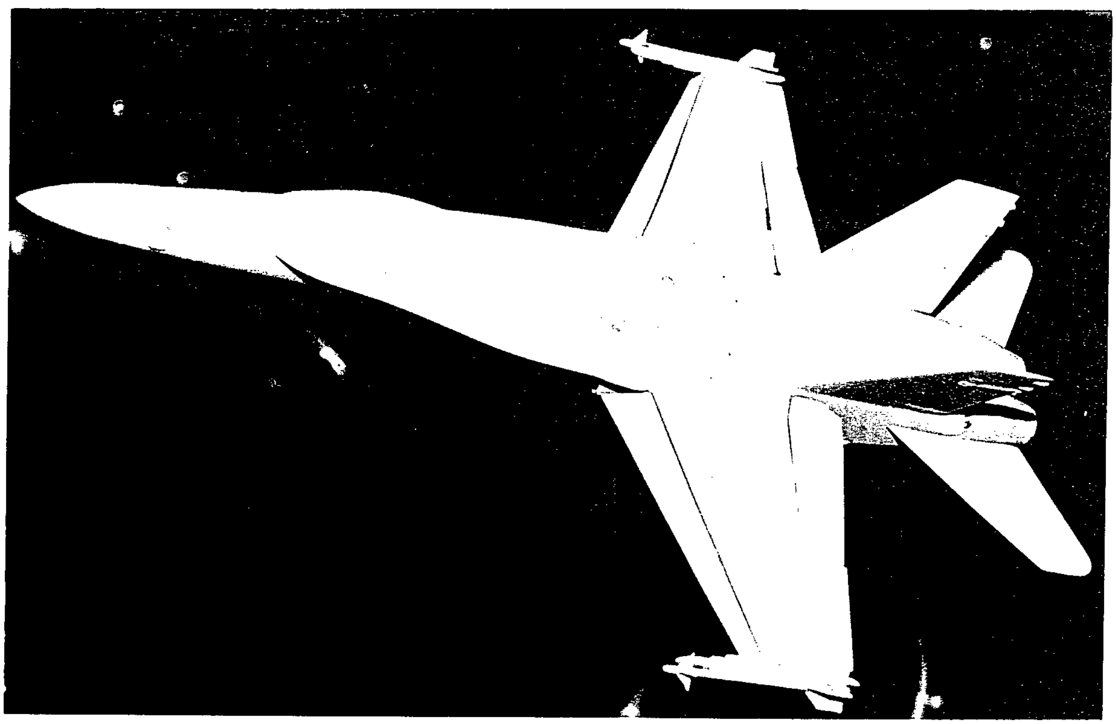

Figure 2. 1/48-scale F/A-18 water tunnel model

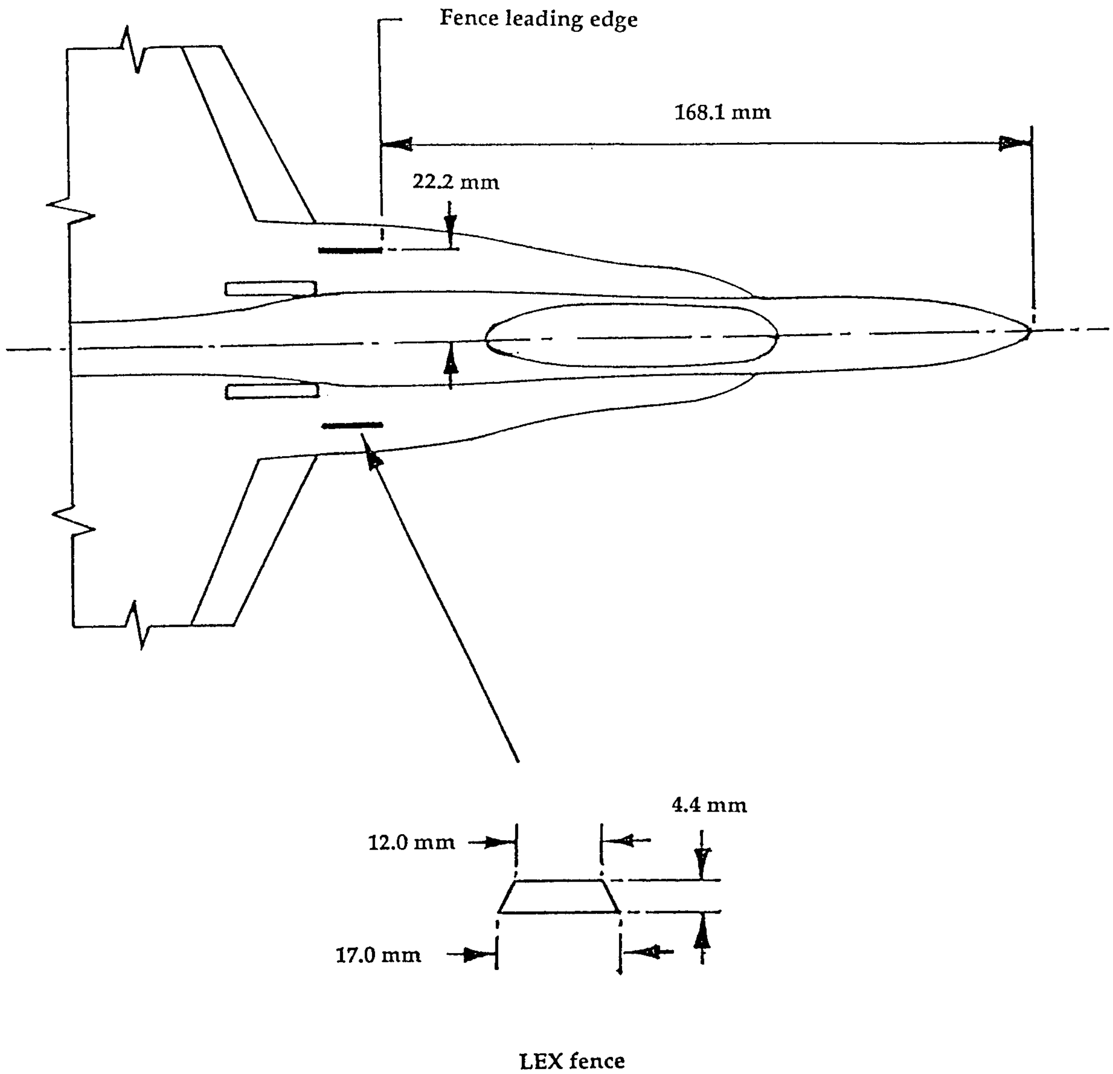

Figure 3. Shape and position of LEX fence on 1/48 scale model

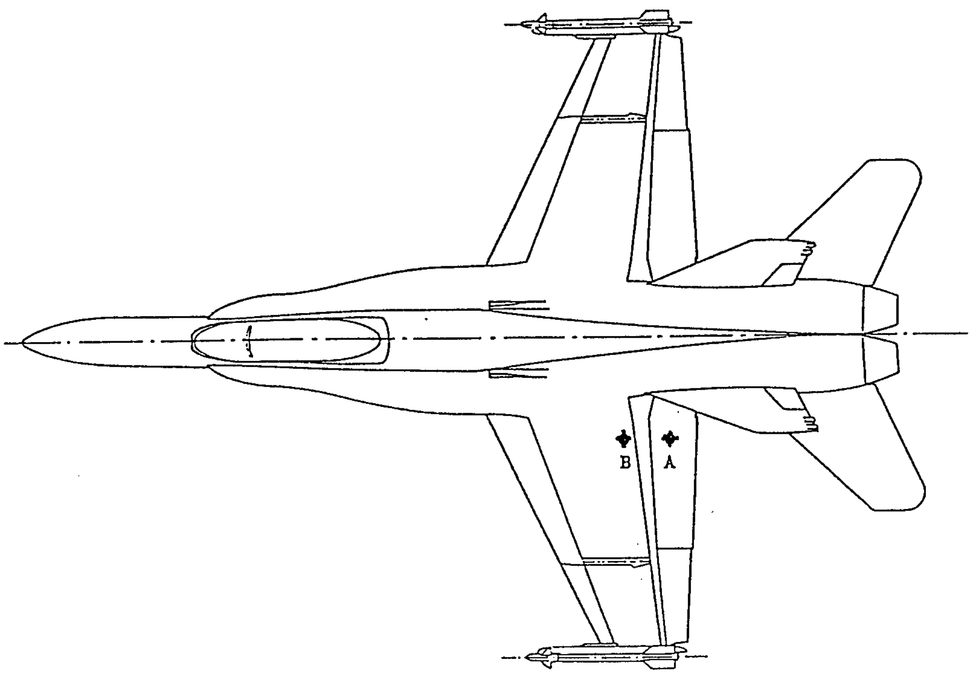

□ Port fin accelerometer;
60% chord, 93% span

○ Port fin differential pressure tappings;
10% chord, 30, 60, and 90% span

● Port fin outboard pressure tapping;
64% chord, 90% span

✦ Wing surface mounted pressure transducers;
31% span port of A/C centreline,
71.8% (A) and 66.6% (B) of A/C length

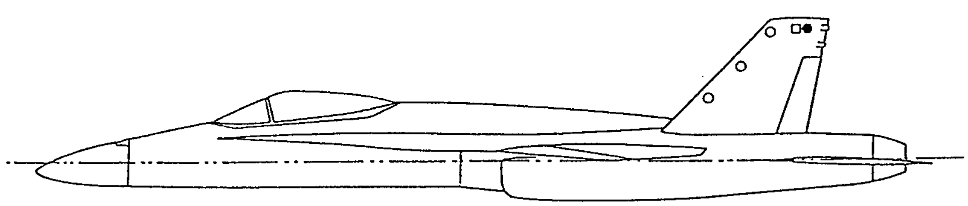

Figure 4. Location of pressure transducers and accelerometers on 1/9-scale F/A-18 wind tunnel model

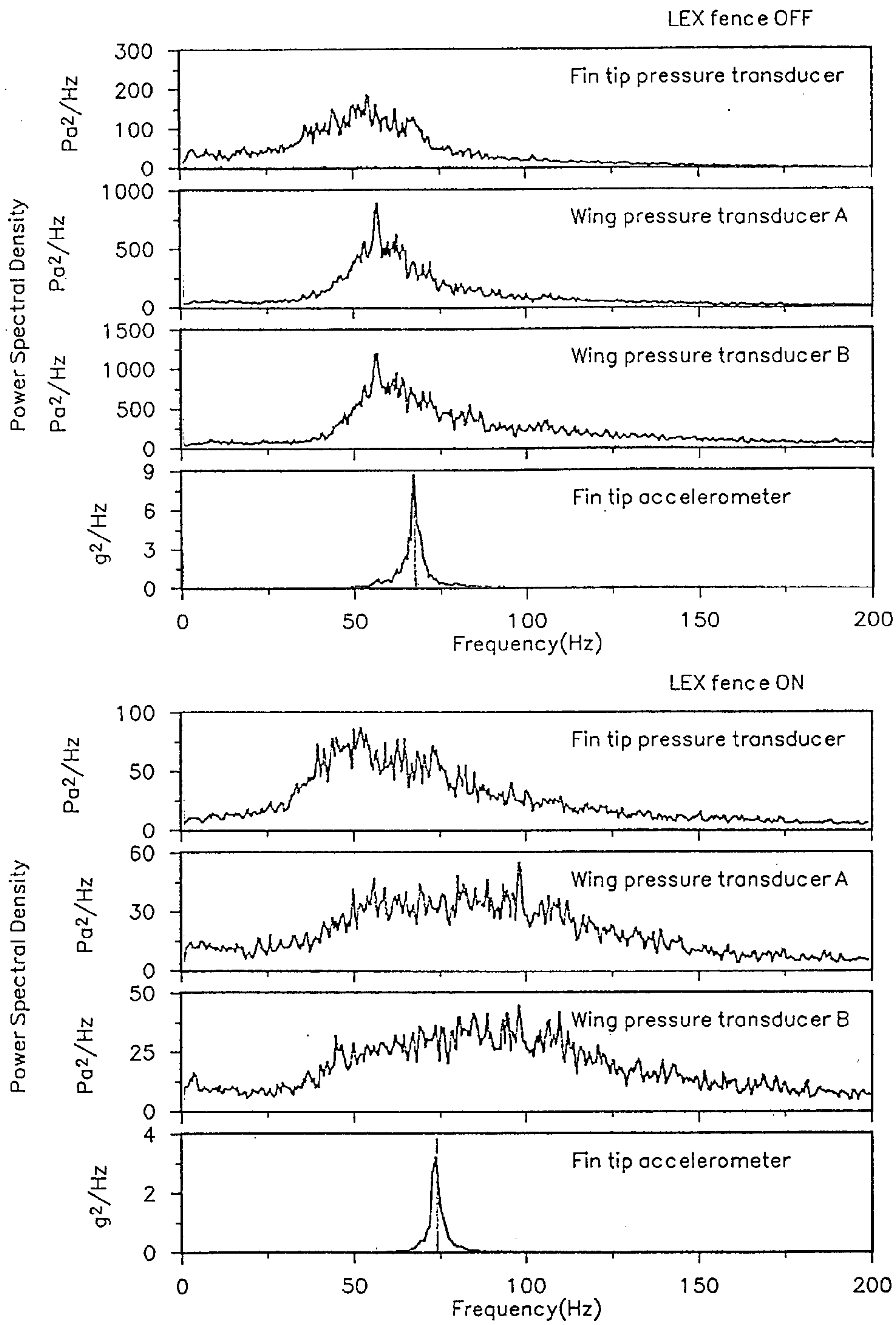

Figure 5(a). Power spectral density results for wind tunnel at airspeed = 30 m/s (Angle of attack = 25.4°; leading-edge flap deflection = 35°; trailing-edge flap deflection = 0°)

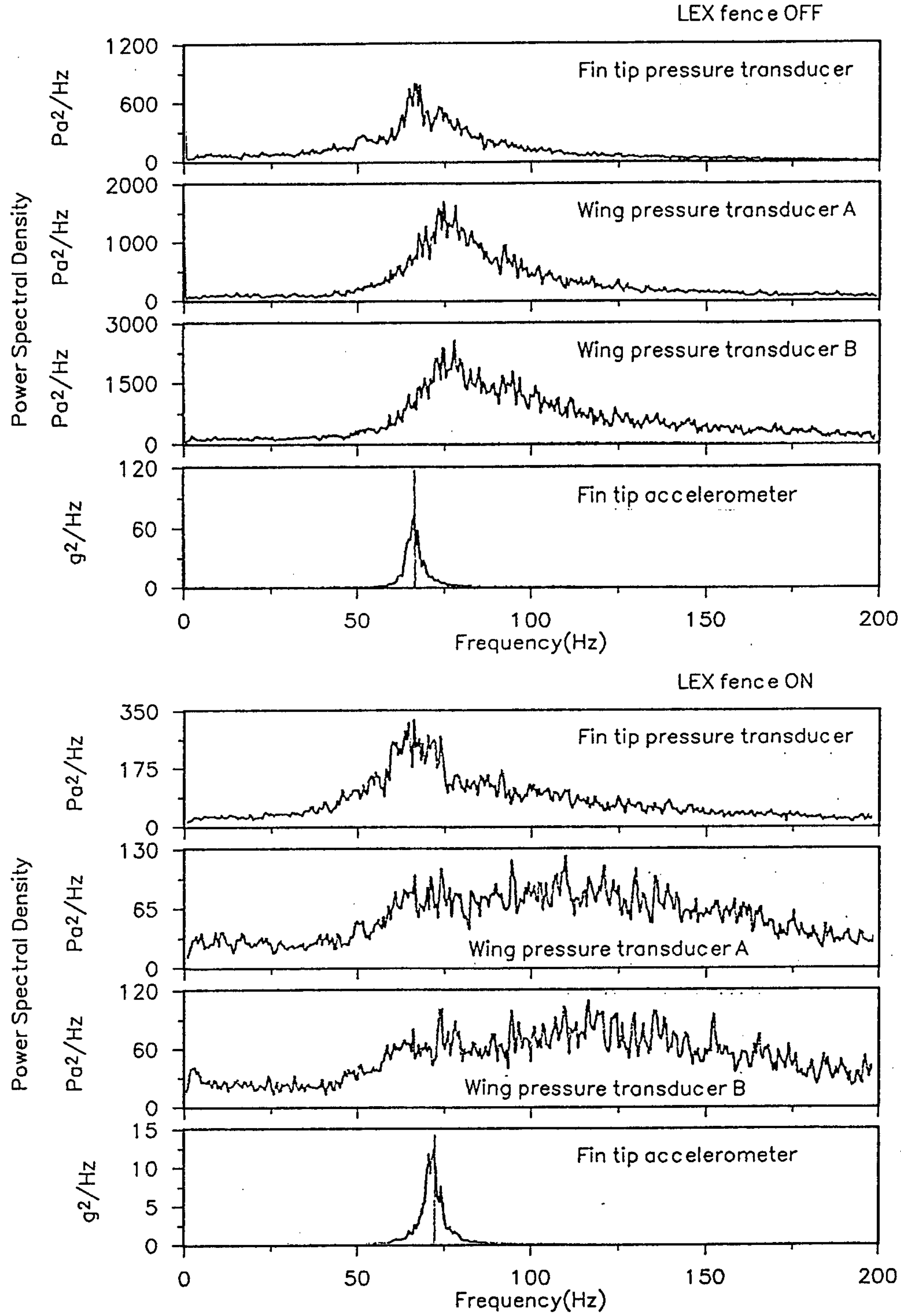

Figure 5(b). Power spectral density results for wind tunnel at airspeed = 40 m/s (Angle of attack = 25.4°; leading-edge flap deflection = 35°; trailing-edge flap deflection = 0°)

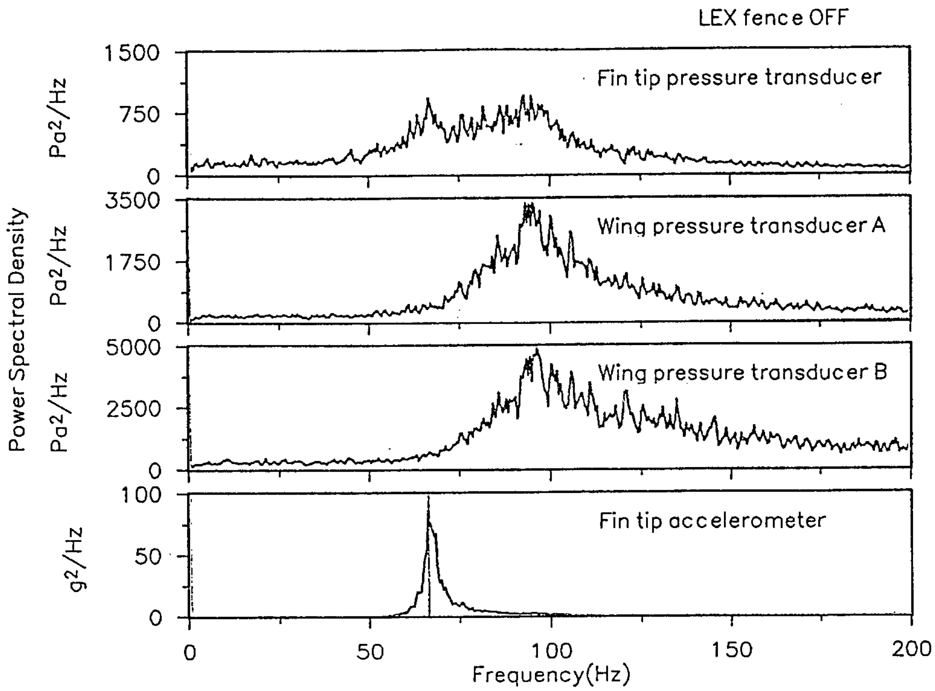

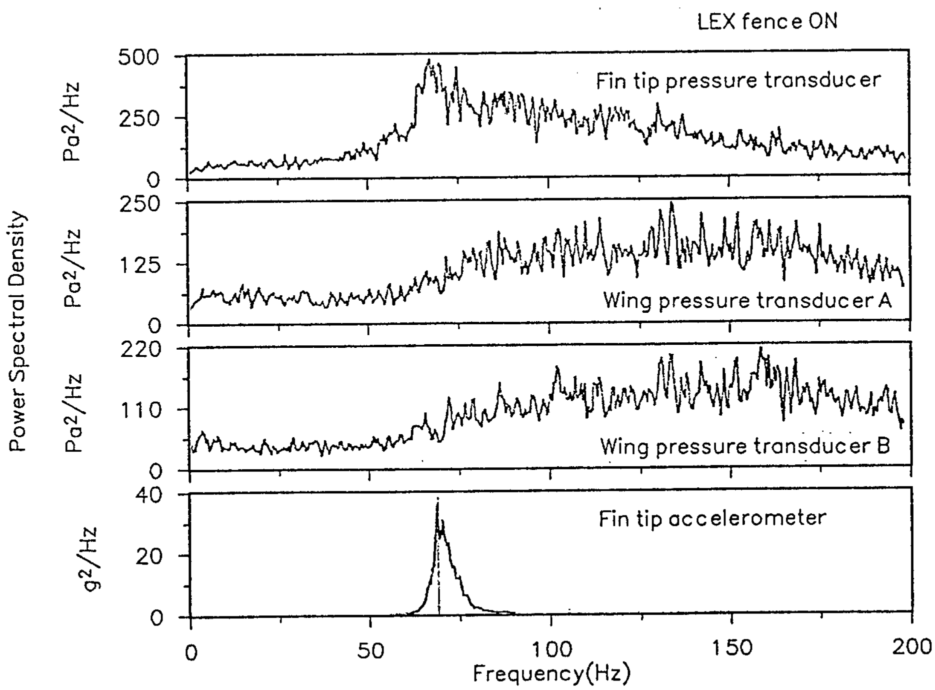

Figure 5(c). Power spectral density results for wind tunnel at airspeed = 50 m/s (Angle of attack = 25.4°; leading-edge flap deflection = 35°; trailing-edge flap deflection = 0°)

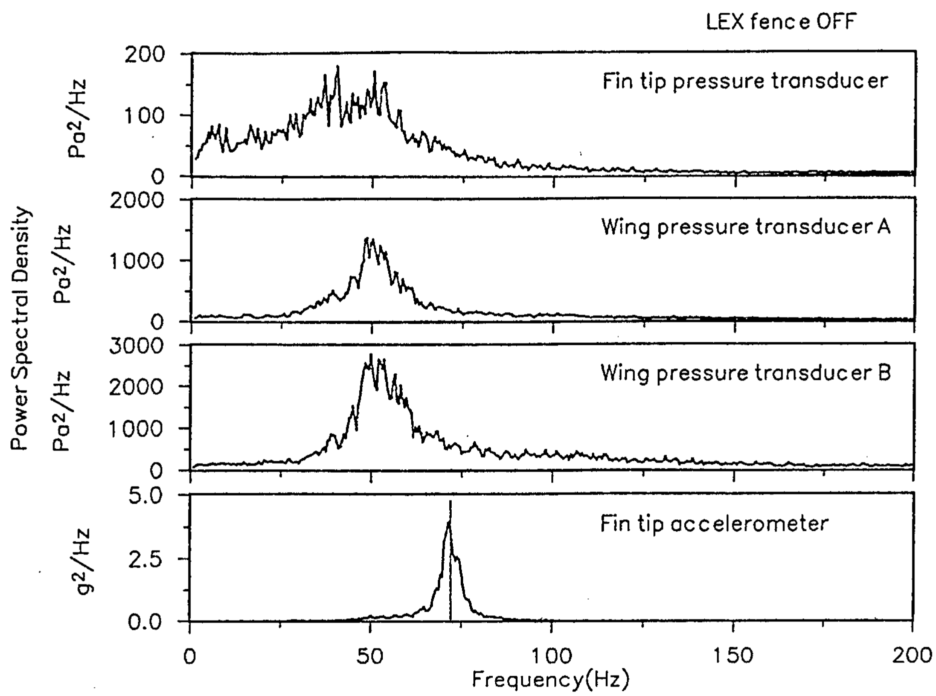

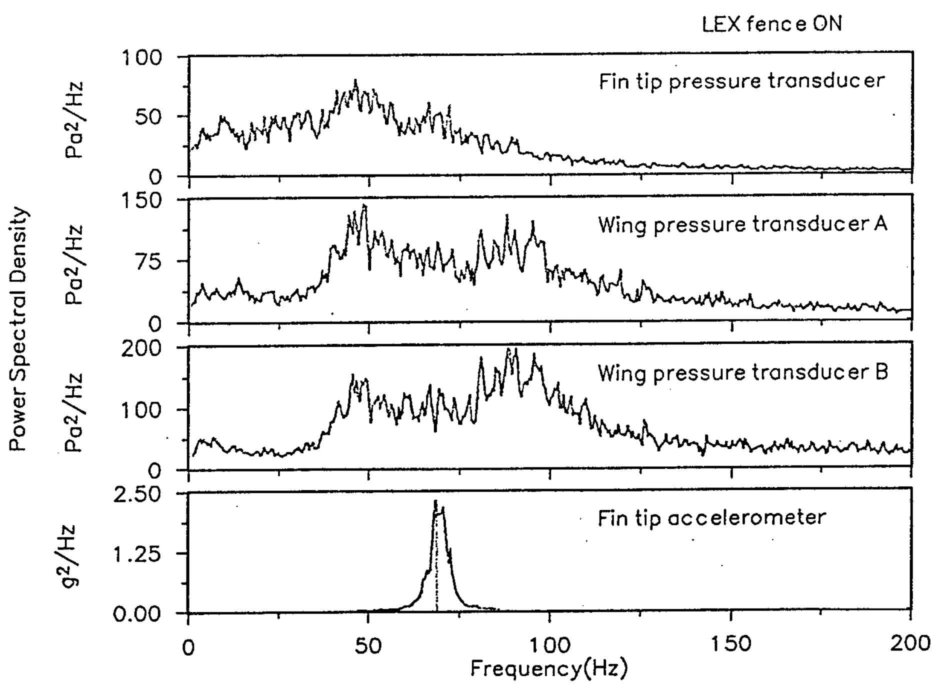

Figure 6(a). Power spectral density results for wind tunnel at airspeed = 30 m/s (Angle of attack = 30.5°; leading-edge flap deflection = 35°; trailing-edge flap deflection = 0°)

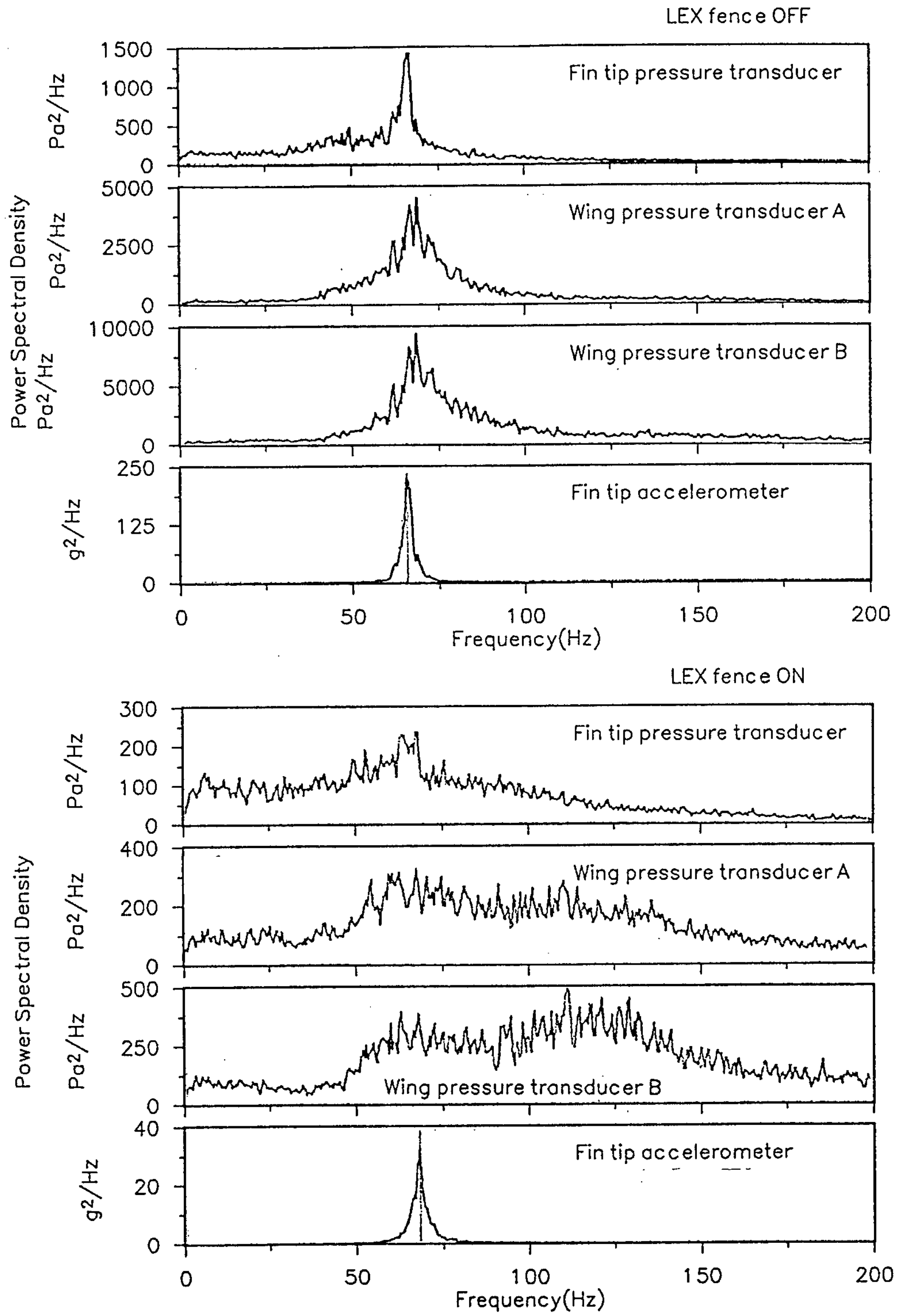

Figure 6(b). Power spectral density results for wind tunnel at airspeed = 40 m/s (Angle of attack = 30.5°; leading-edge flap deflection = 35°; trailing-edge flap deflection = 0°)

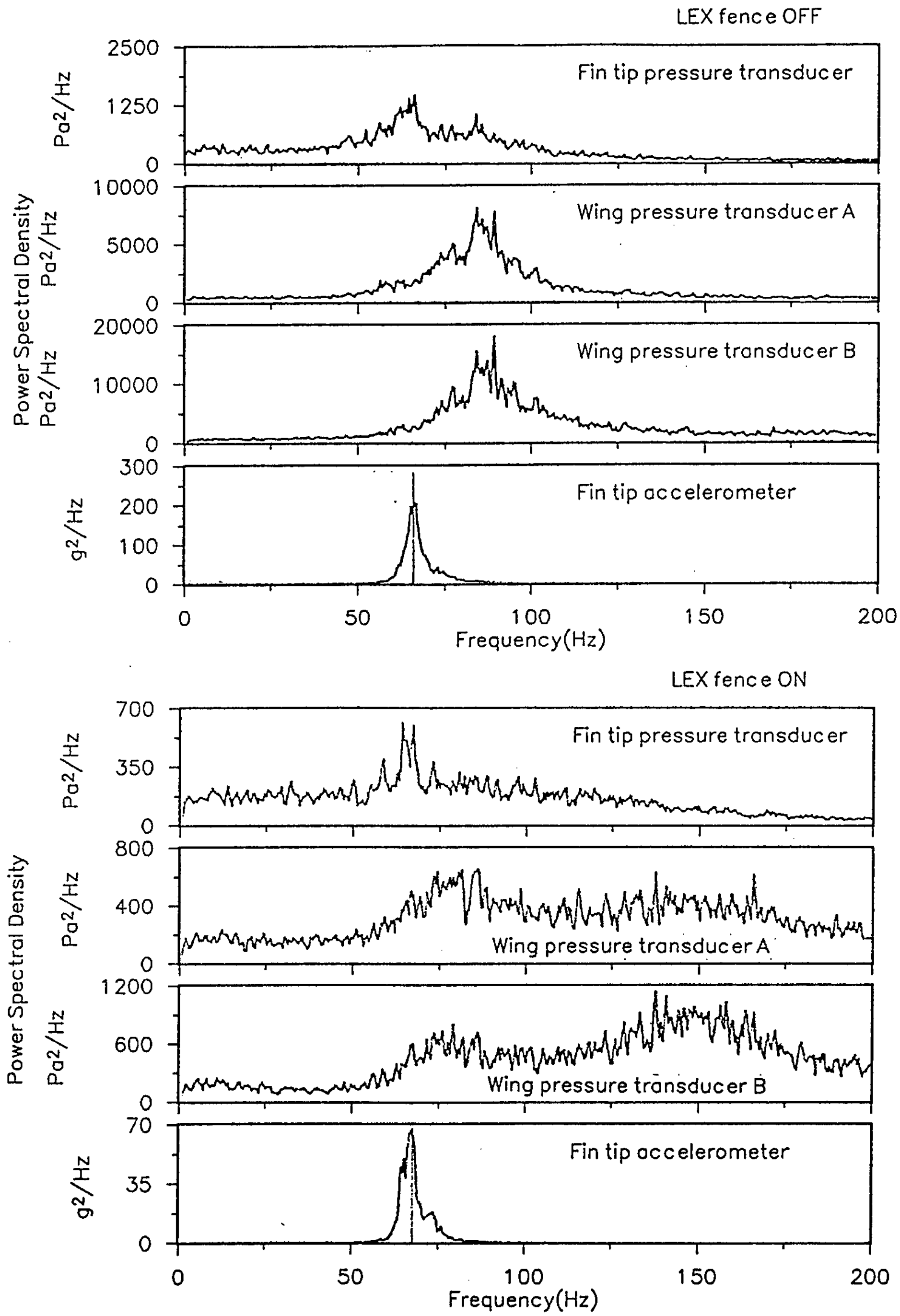

Figure 6(c). Power spectral density results for wind tunnel at airspeed = 50 m/s (Angle of attack = 30.5°; leading-edge flap deflection = 35°; trailing-edge flap deflection = 0°)

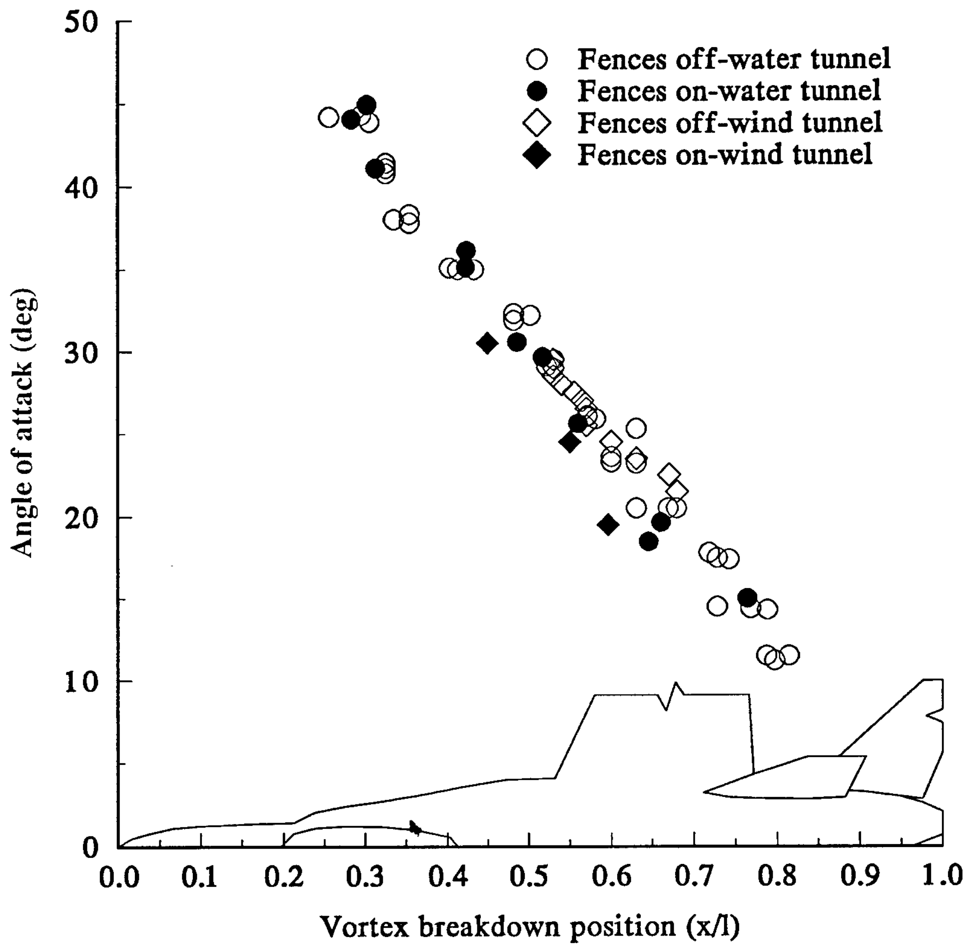

Figure 7. Effect of LEX fences on vortex breakdown position over F/A-18 model (Leading-edge flap deflection = 35°; trailing-edge flap deflection = 0°)

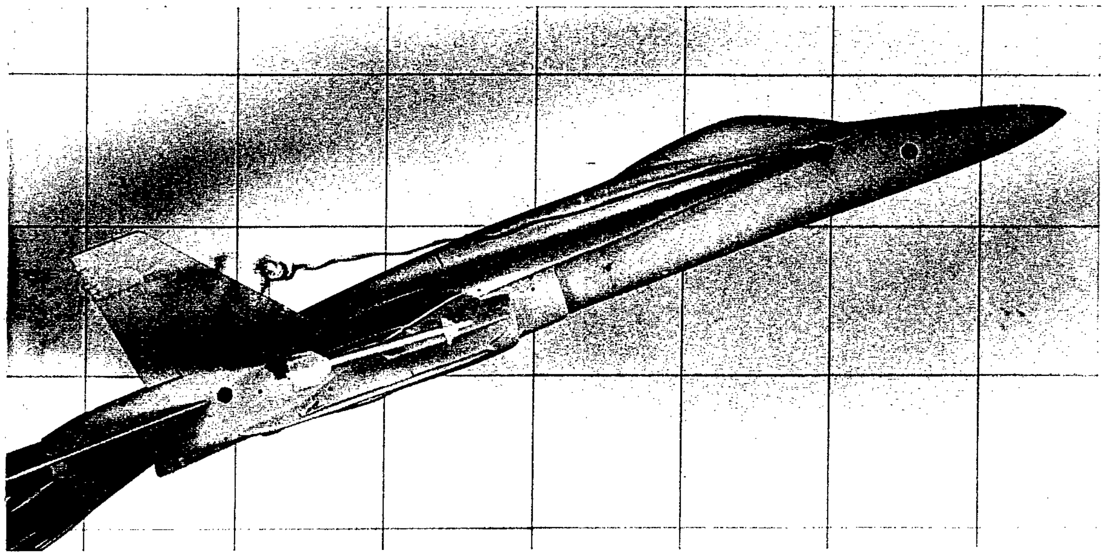

LEX fence off

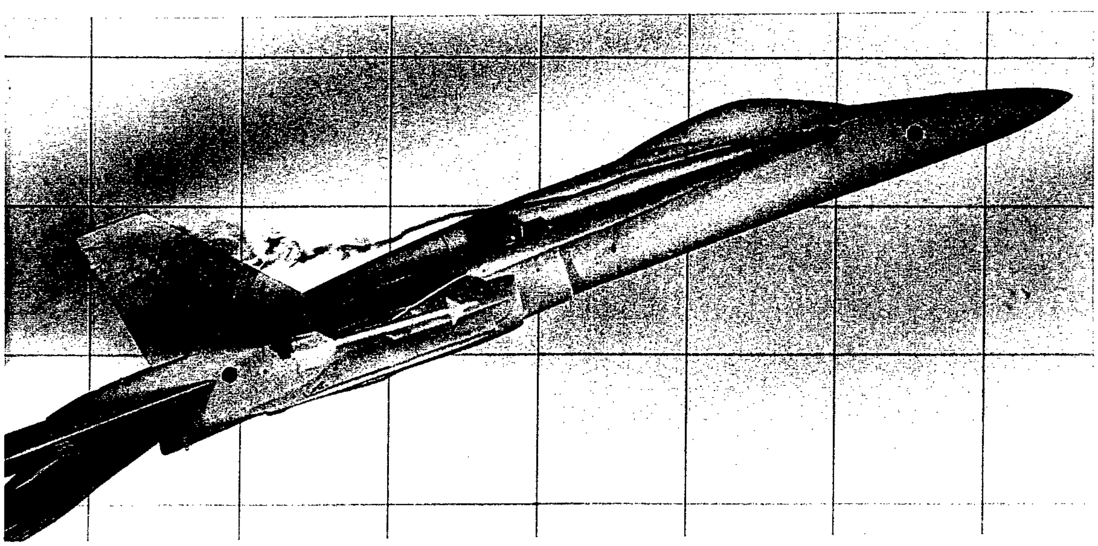

LEX fence on

Figure 8(a). Effect of LEX fence on vortex flow over F/A-18 model in water tunnel (side view) (Angle of attack = 19.5°; leading-edge flap deflection = 35°; trailing-edge flap deflection = 0°; velocity = 80 mm/s)

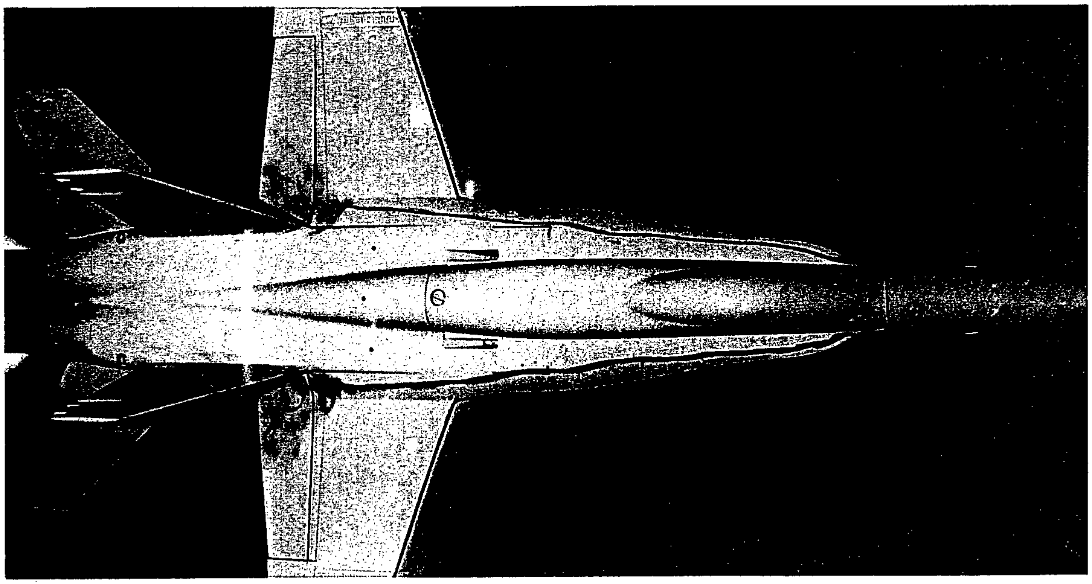

LEX fence off

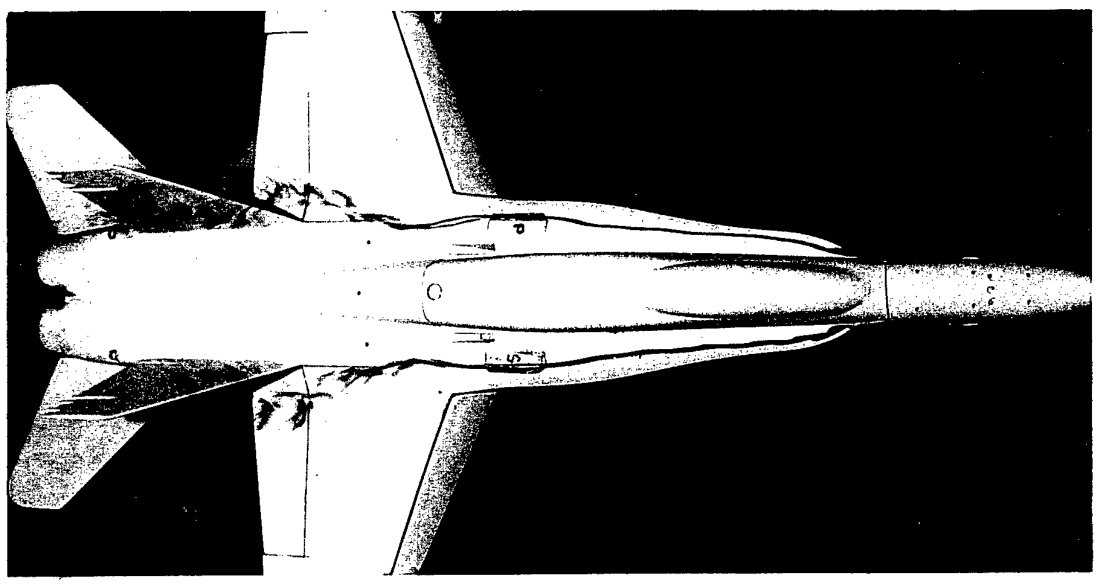

LEX fence on

Figure 8(b). Effect of LEX fence on vortex flow over F/A-18 model in water tunnel (plan view) (Angle of attack = 19.5°; leading-edge flap deflection = 35°; trailing-edge flap deflection = 0°; velocity = 80 mm/s)

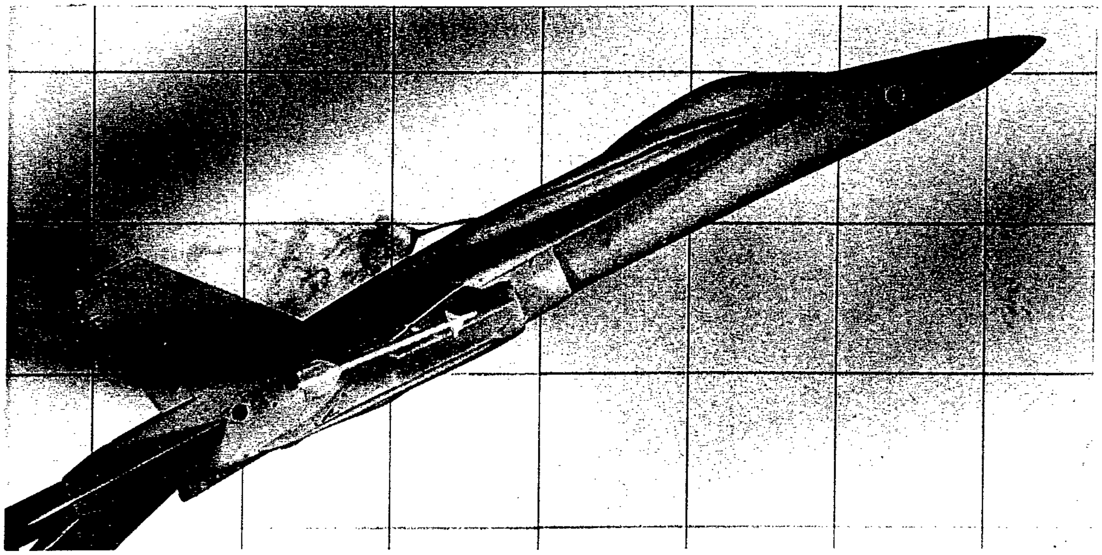

LEX fence off

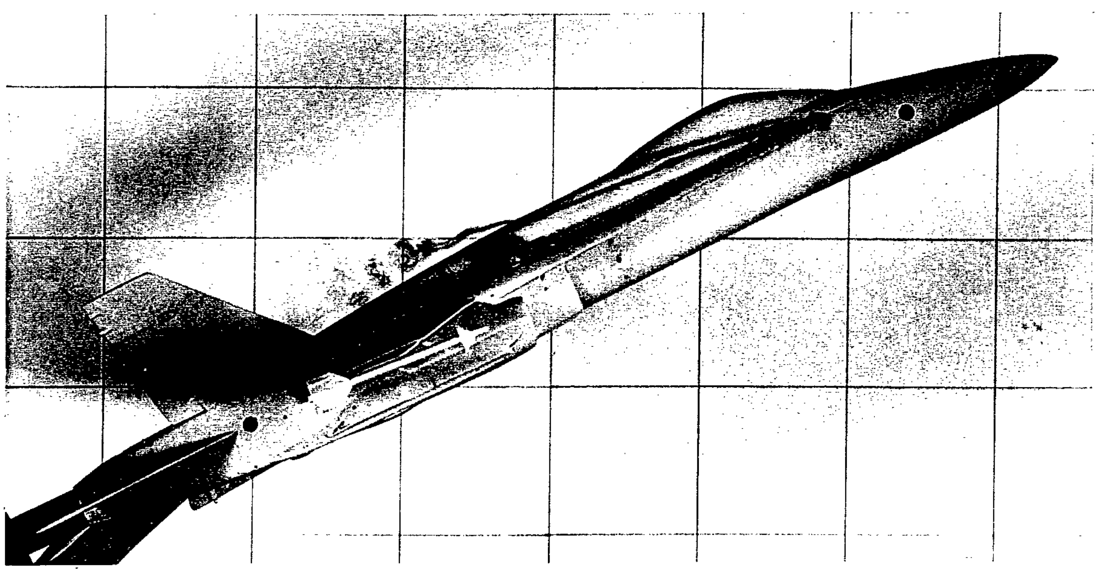

LEX fence on

Figure 8(c). Effect of LEX fence on vortex flow over F/A-18 model in water tunnel (side view) (Angle of attack = 25.4°; leading-edge flap deflection = 35°; trailing-edge flap deflection = 0°; velocity = 80 mm/s)

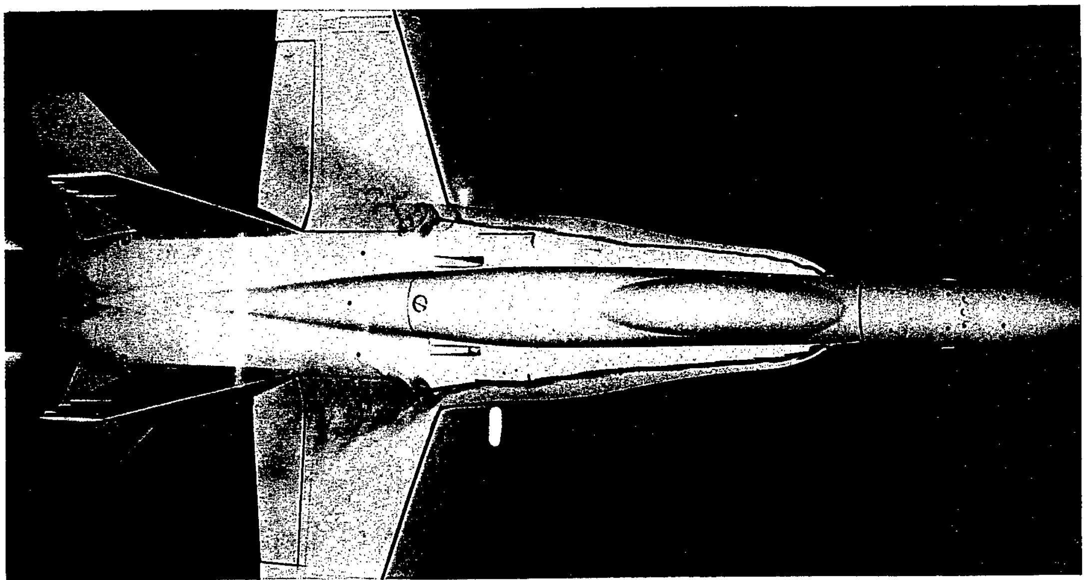

LEX fence off

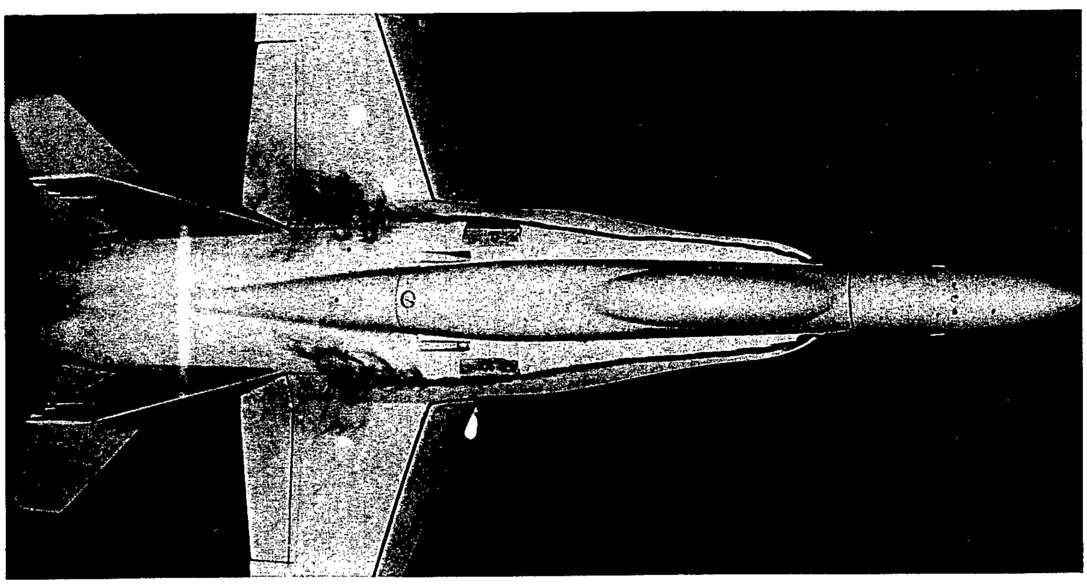

LEX fence on

Figure 8(d). Effect of LEX fence on vortex flow over F/A-18 model in water tunnel (plan view)
(Angle of attack = 25.4°; leading-edge flap deflection = 35°; trailing-edge flap deflection = 0°; velocity = 80 mm/s)

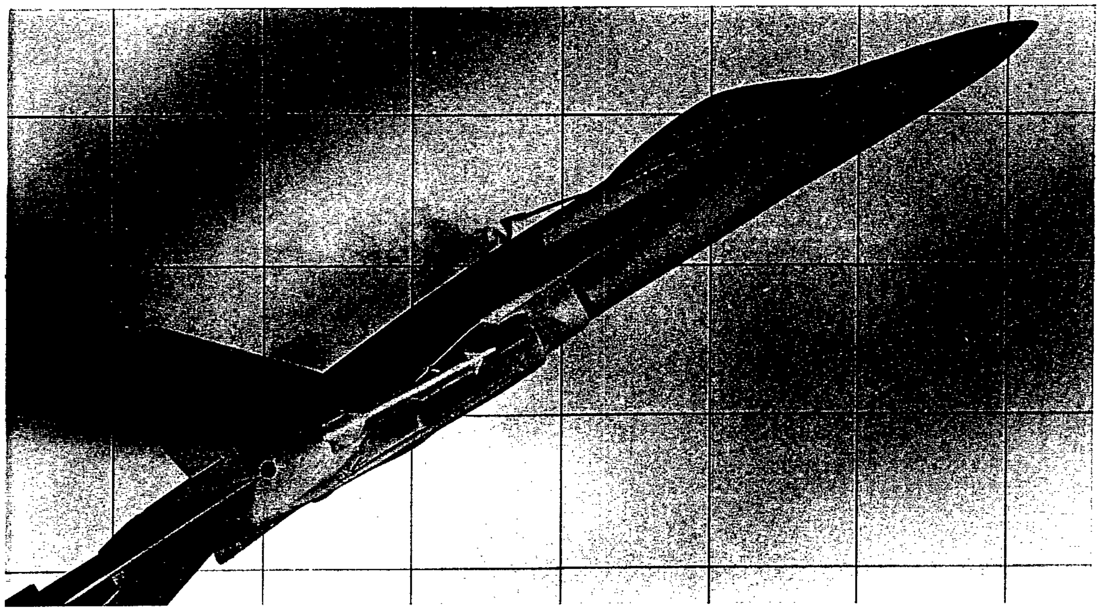

LEX fence off

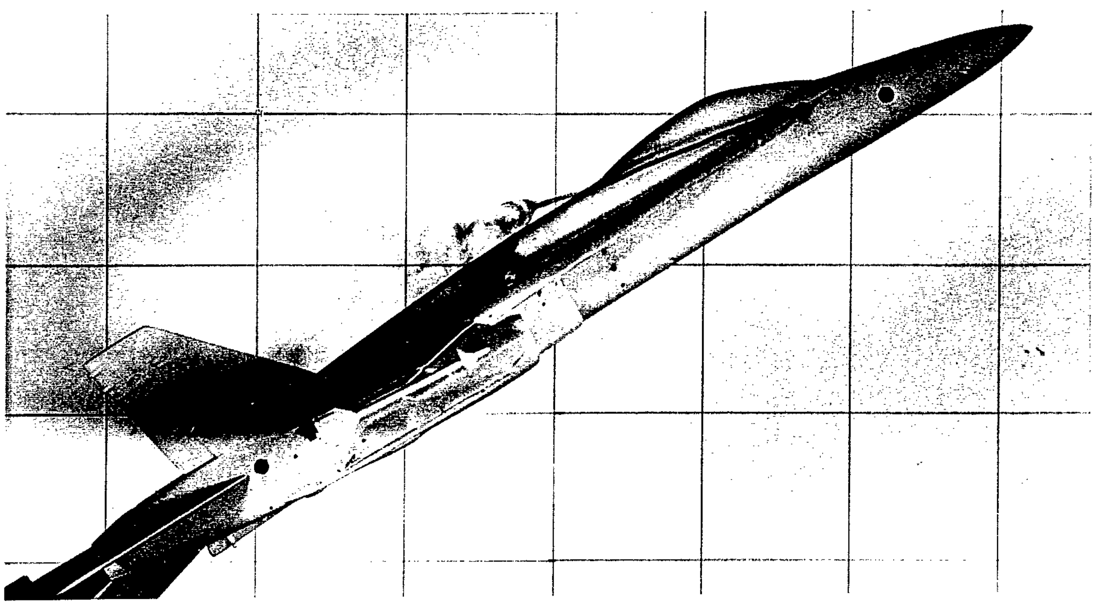

LEX fence on

Figure 8(e). Effect of LEX fence on vortex flow over F/A-18 model in water tunnel (side view) (Angle of attack = 30.5°; leading-edge flap deflection = 35°; trailing-edge flap deflection = 0°; velocity = 80 mm/s)

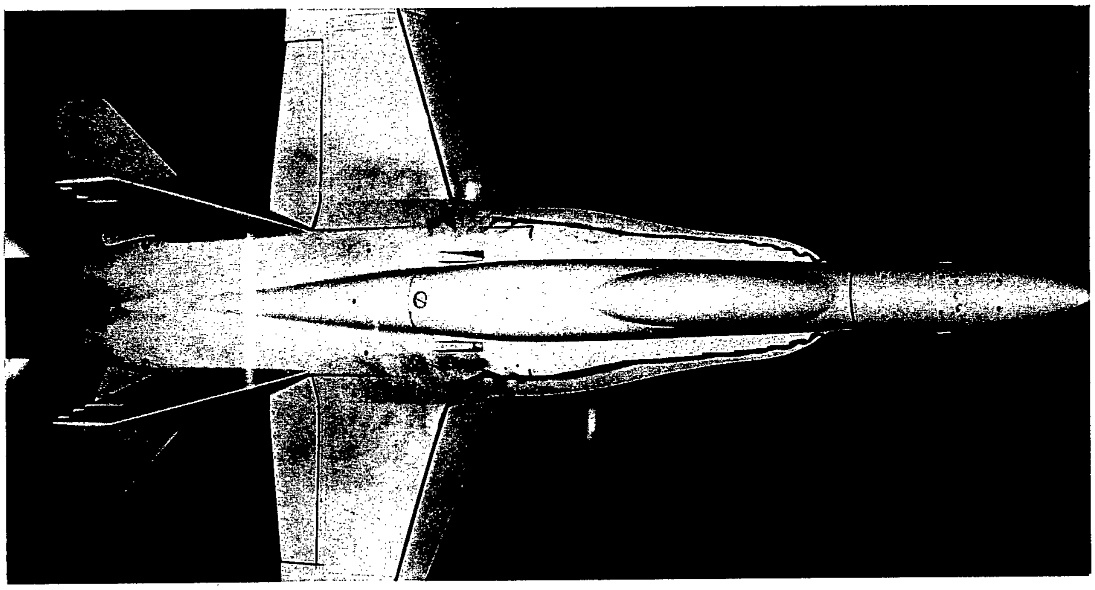

LEX fence off

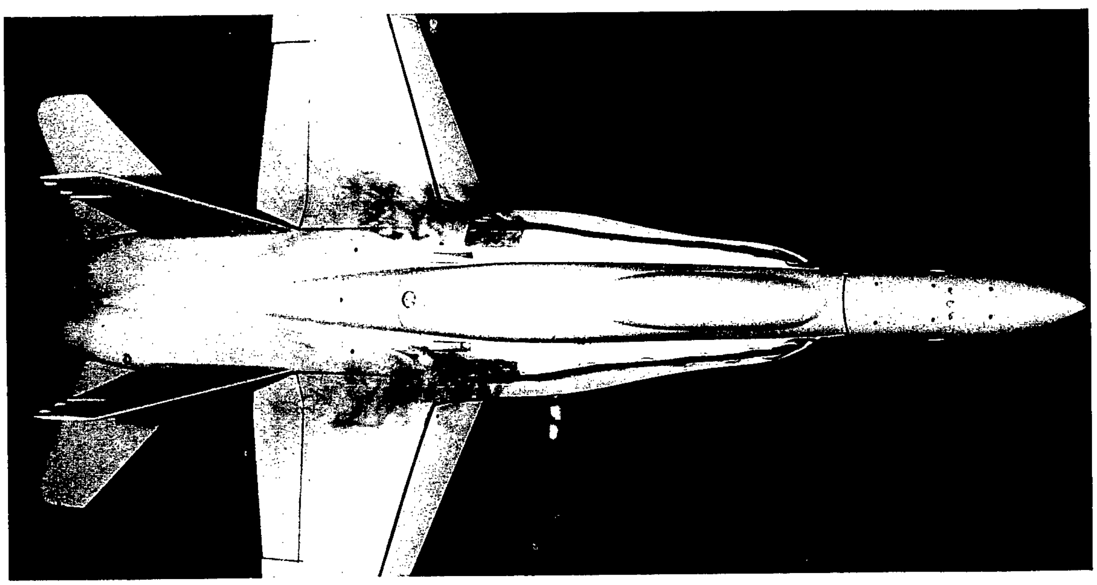

LEX fence on

Figure 8(f). Effect of LEX fence on vortex flow over F/A-18 model in water tunnel (plan view) (Angle of attack = 30.5°; leading-edge flap deflection = 35°; trailing-edge flap deflection = 0°; velocity = 80 mm/s)

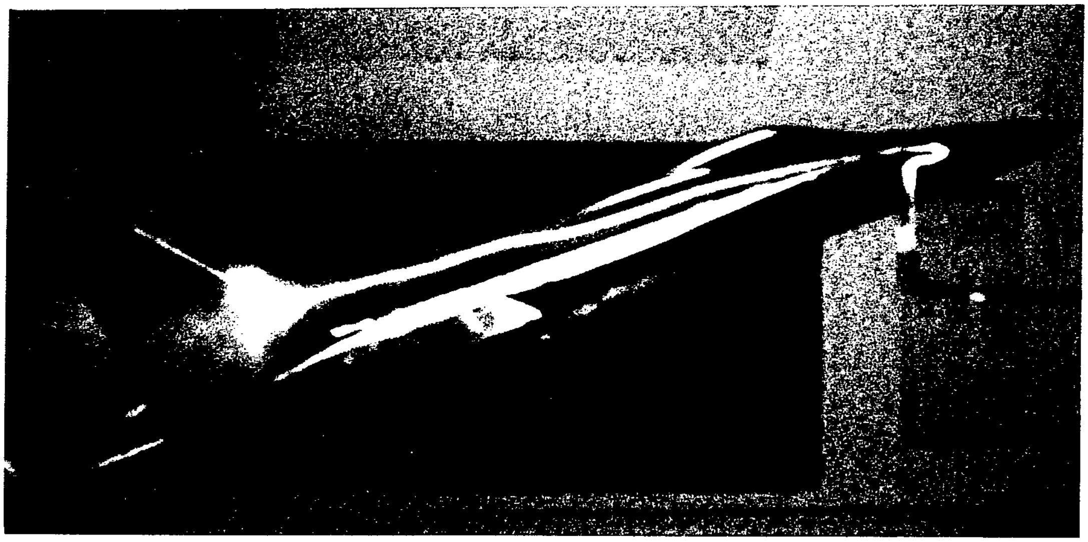

LEX fence off

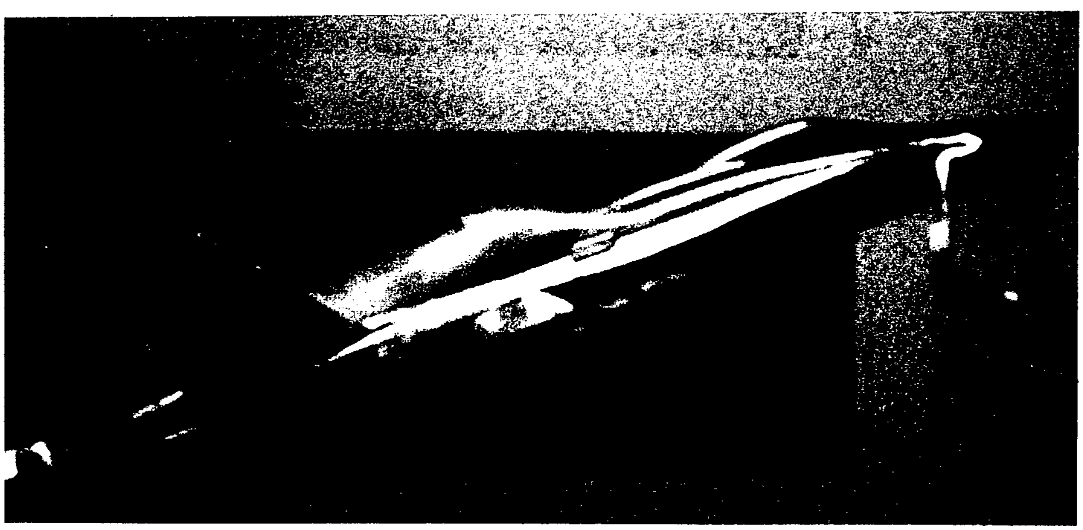

LEX fence on

Figure 9(a). Effect of LEX fence on vortex flow over F/A-18 model in wind tunnel (side view) (Angle of attack = 19.5°; leading-edge flap deflection = 35°; trailing-edge flap deflection = 0°; velocity = 5 m/s)

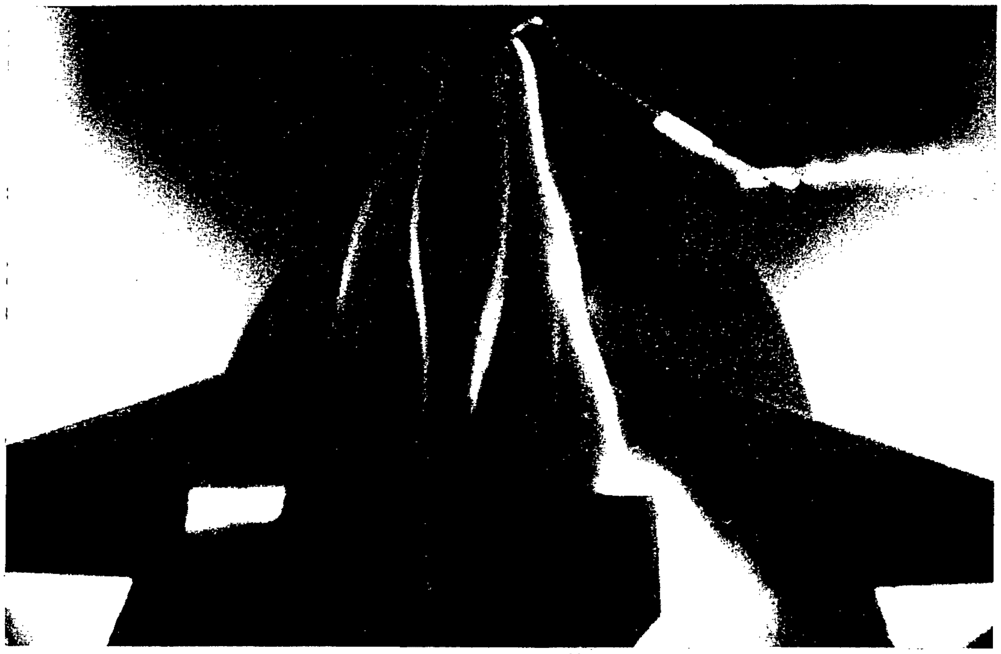

LEX fence off

LEX fence on

Figure 9(b). Effect of LEX fence on vortex flow over F/A-18 model in wind tunnel (rear view)
(Angle of attack = 19.5°; leading-edge flap deflection = 35°; trailing-edge flap deflection = 0°; velocity = 5 m/s)

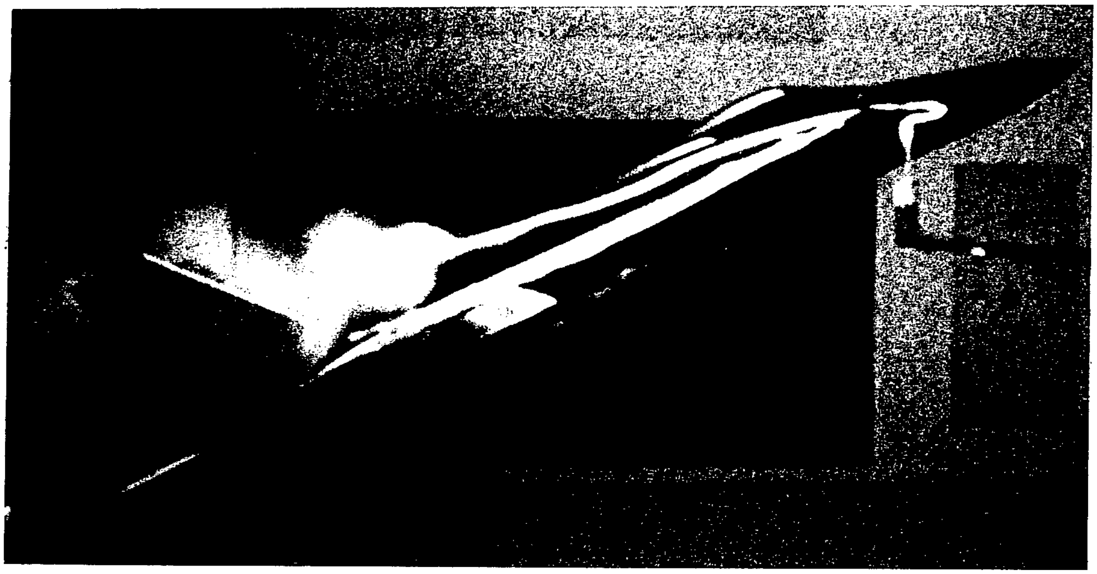

LEX fence off

LEX fence on

Figure 9(c). Effect of LEX fence on vortex flow over F/A-18 model in wind tunnel (side view) (Angle of attack = 25.4°; leading-edge flap deflection = 35°; trailing-edge flap deflection = 0°; velocity = 5 m/s)

LEX fence off

LEX fence on

Figure 9(d). Effect of LEX fence on vortex flow over F/A-18 model in wind tunnel (rear view) (Angle of attack = 25.4°; leading-edge flap deflection = 35°; trailing-edge flap deflection = 0°; velocity = 5 m/s)

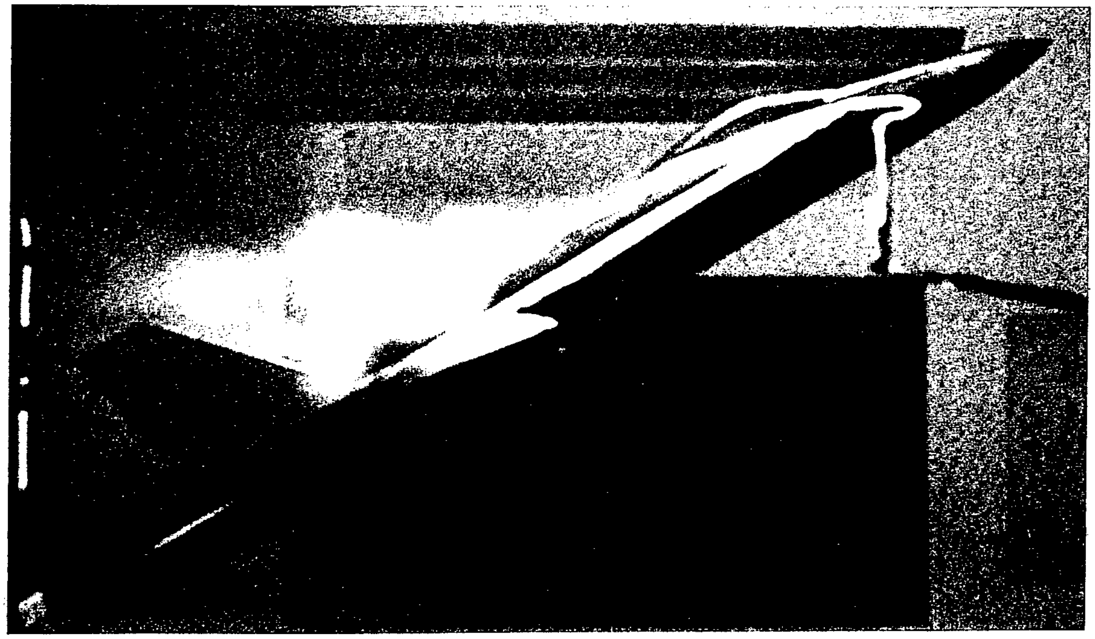

LEX fence off

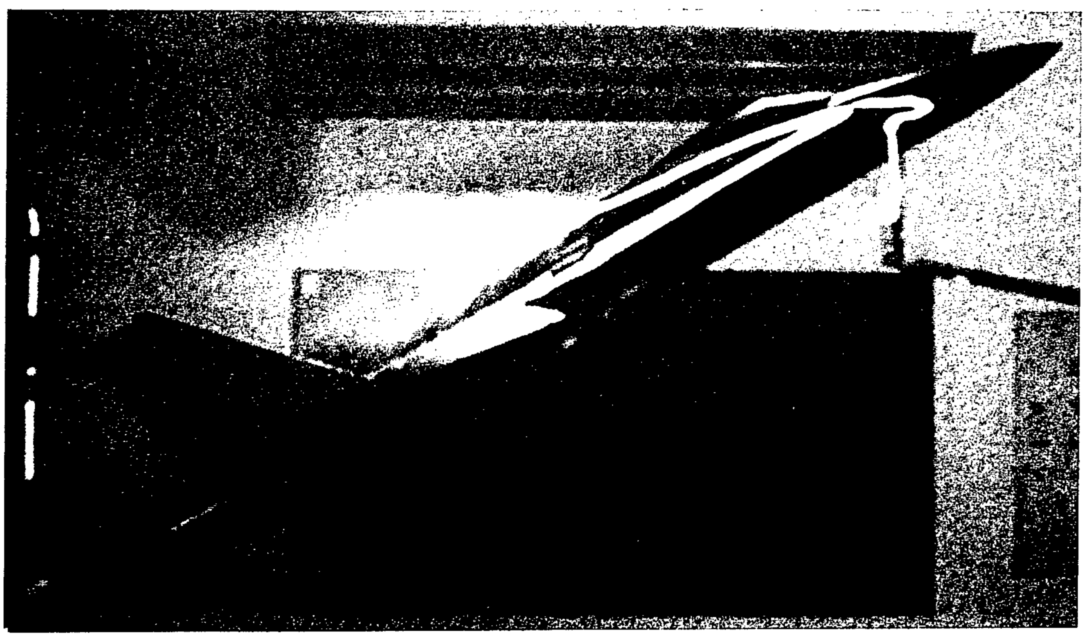

LEX fence on

Figure 9(e). Effect of LEX fence on vortex flow over F/A-18 model in wind tunnel (side view) (Angle of attack = 30.5°; leading-edge flap deflection = 35°; trailing-edge flap deflection = 0°; velocity = 5 m/s)

LEX fence off

LEX fence on

Figure 9(f). Effect of LEX fence on vortex flow over F/A-18 model in wind tunnel (rear view)
(Angle of attack = 30.5°; leading-edge flap deflection = 35°; trailing-edge flap deflection = 0°; velocity = 5 m/s)

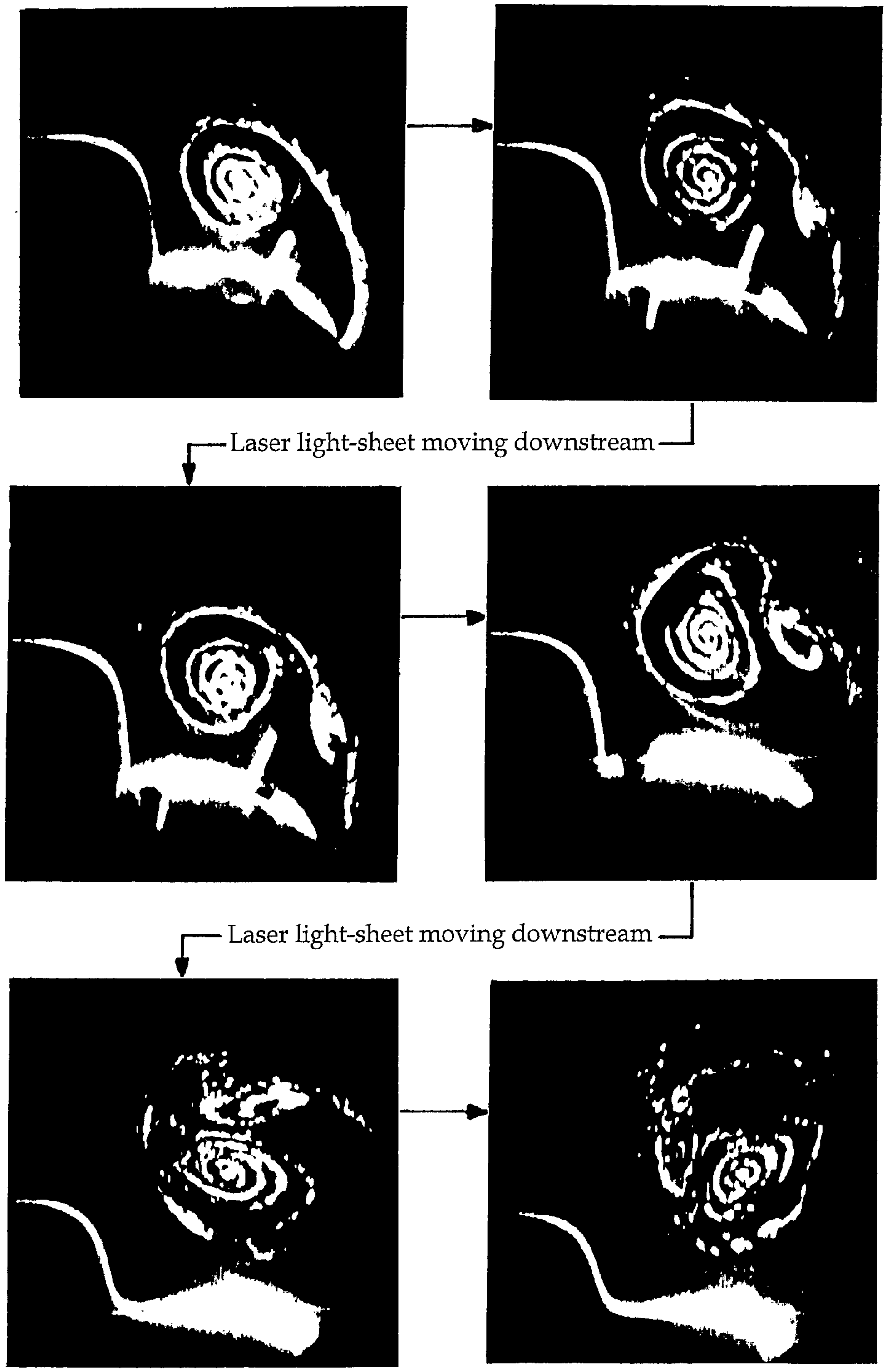

Figure 10(a). Cross-sections of LEX vortex system near fence, visualised using hydrogen bubbles and laser light-sheet

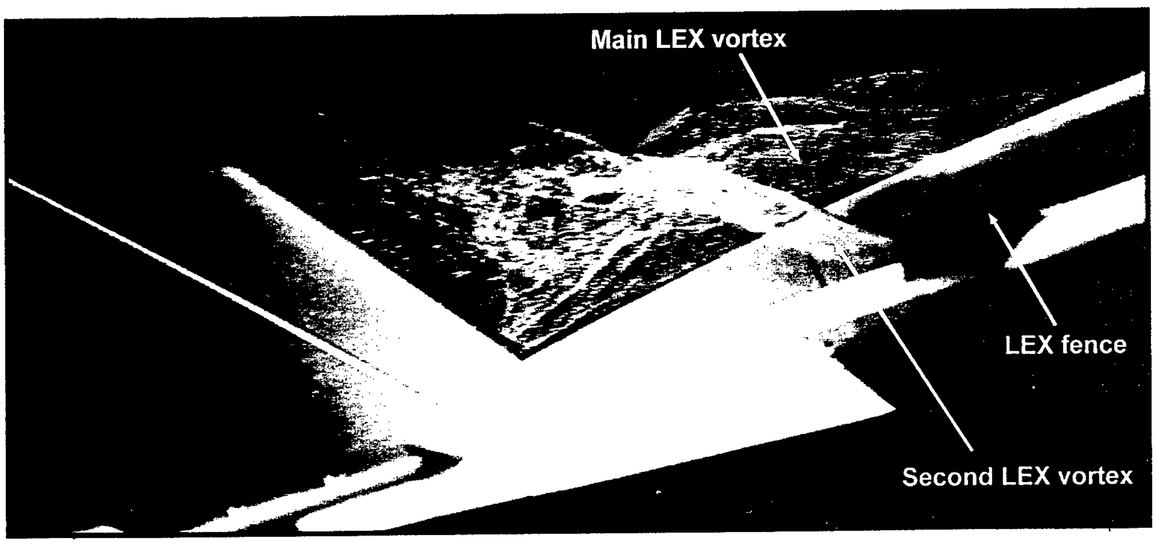

Figure 10(b). Main and second LEX vortices visualised using hydrogen bubbles

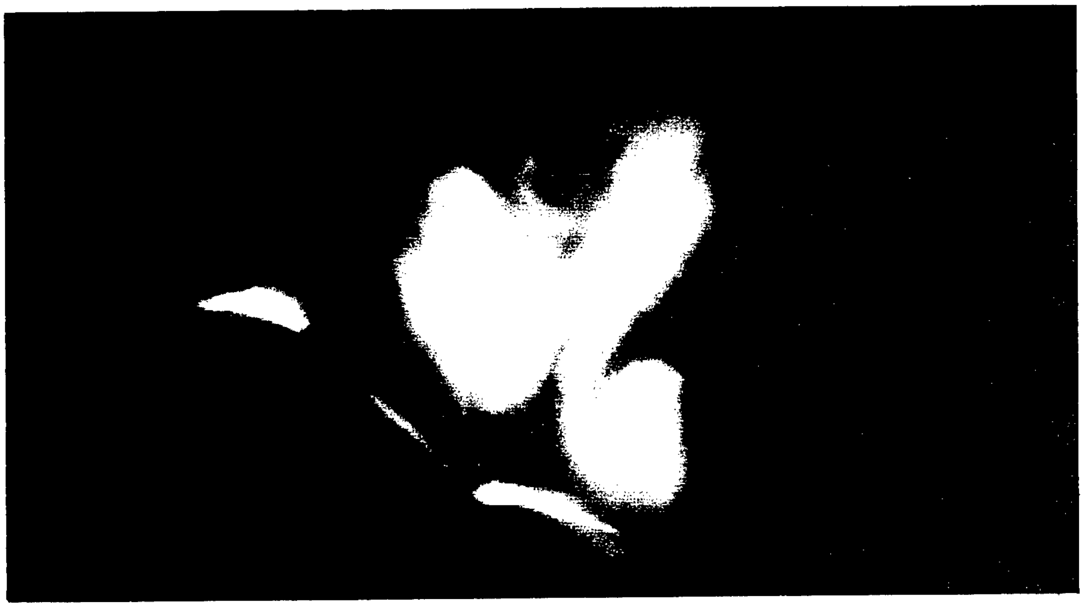

(a) Image direct from videotape

(b) Image with filtering and edge enhancement

Figure 11. Cross-sections of vortex system near LEX fence, visualised using smoke and laser light-sheet

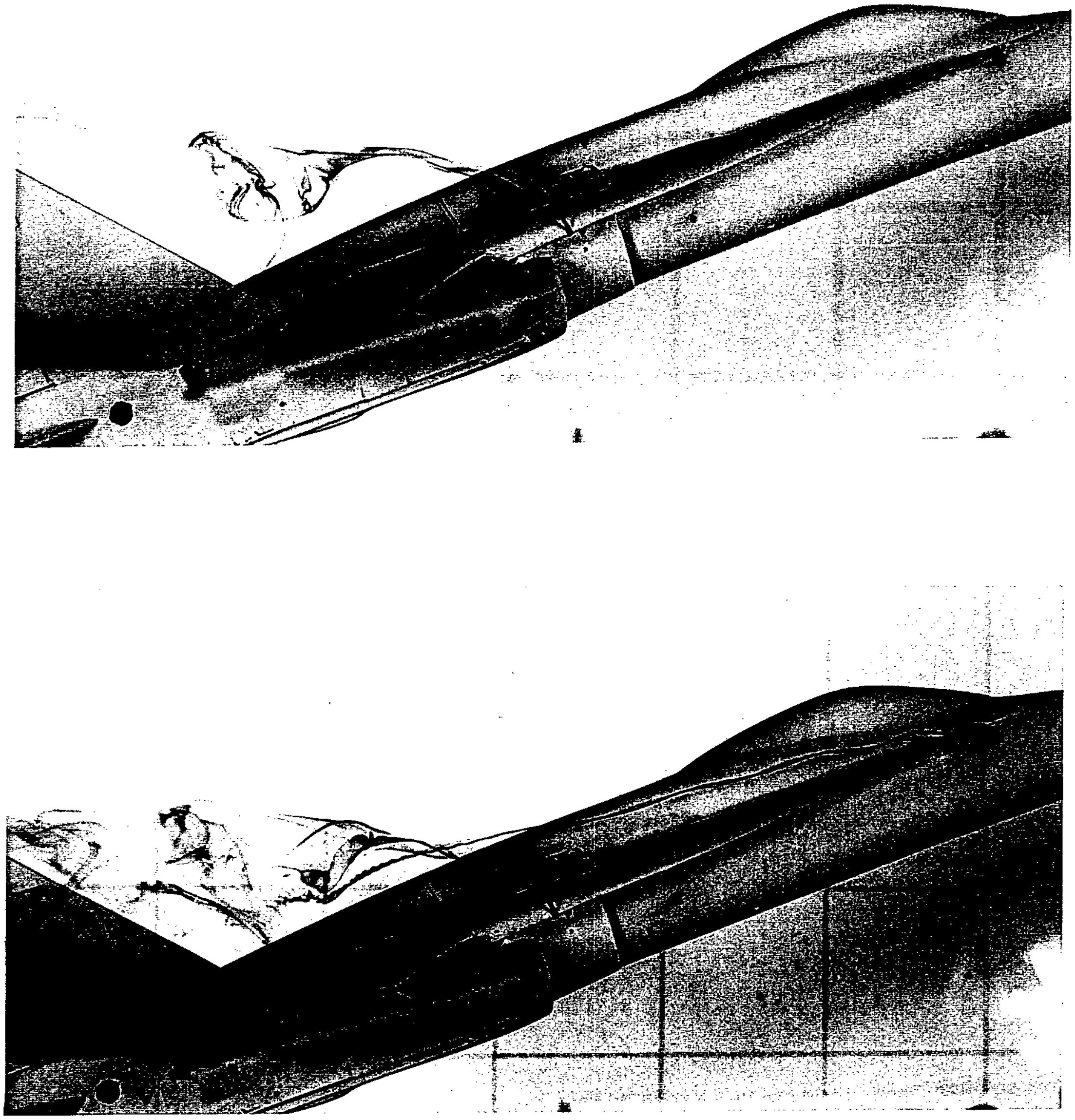

Figure 12. Breakdown in second vortex with fences on (Angle of attack = 19.5°; leading-edge flap deflection = 35°; trailing-edge flap deflection = 0°; velocity = 30 mm/s)

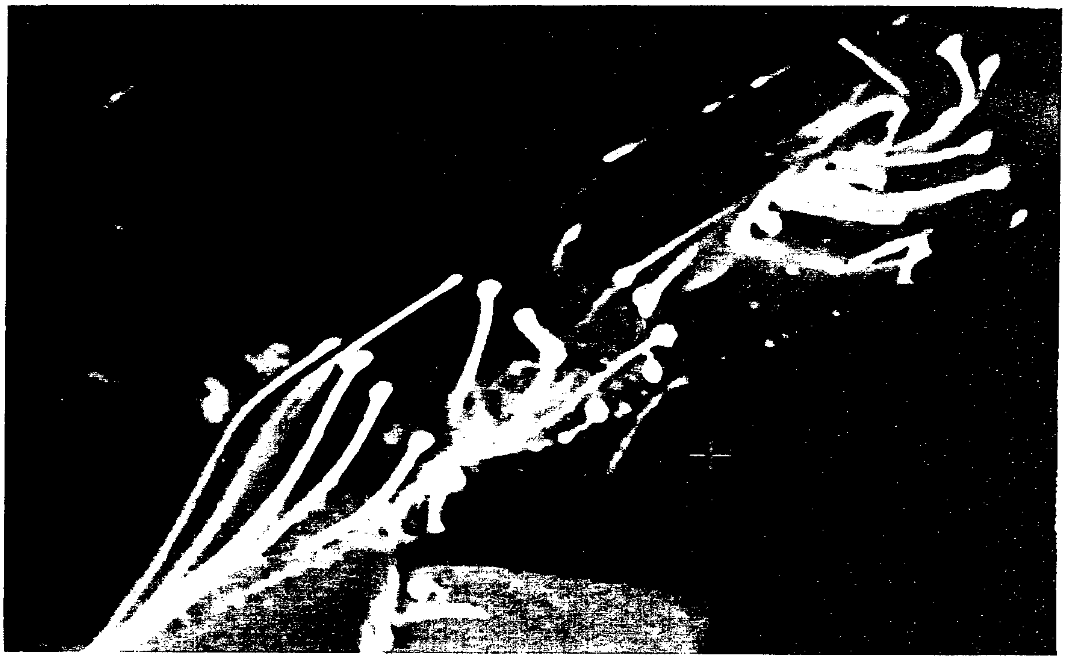

(a) Pattern of dye lines from paste dots

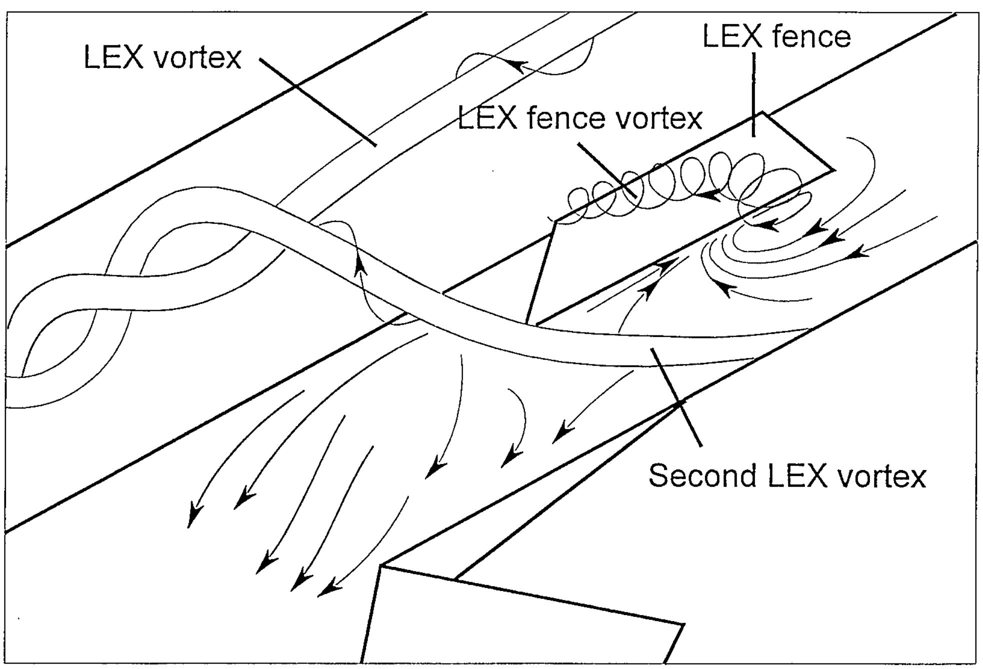

(b) Sketch of flow pattern near LEX fence

Figure 13. Flow patterns outboard of LEX fence
(Angle of attack = 19.5°; leading-edge flap deflection = 35°;
trailing-edge flap deflection = 0°; velocity = 80 mm/s)

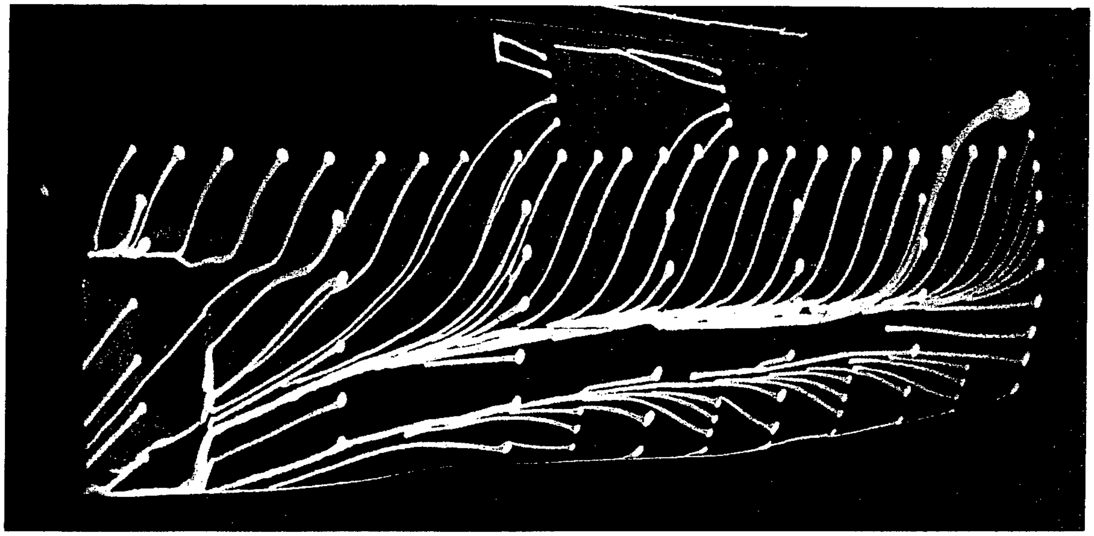

LEX fence off

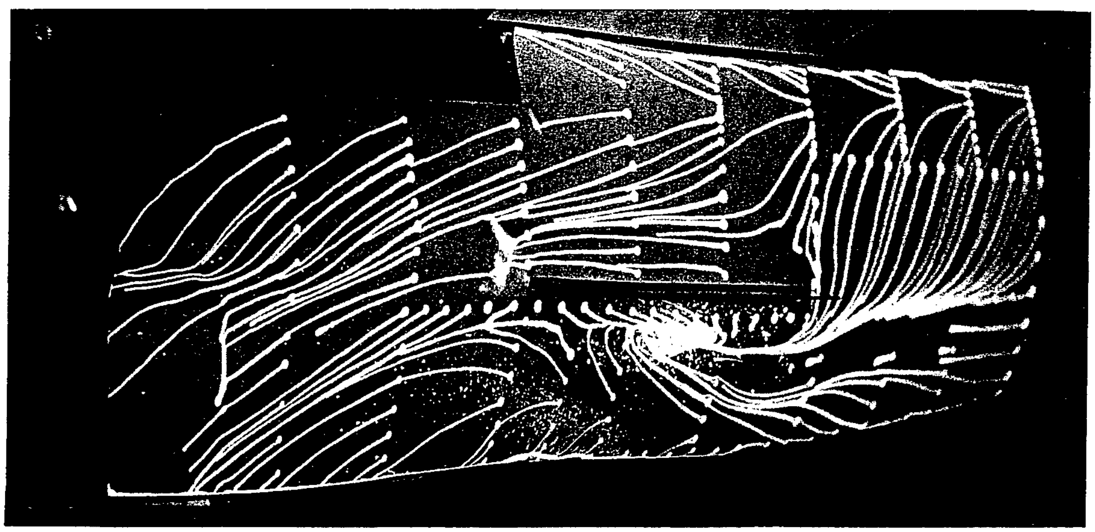

LEX fence on

Figure 14(a). Surface flow pattern near fence on LEX upper surface of wind tunnel model (Angle of attack = 19.5°; leading-edge flap deflection = 35°; trailing-edge flap deflection = 0°; velocity = 50 m/s)

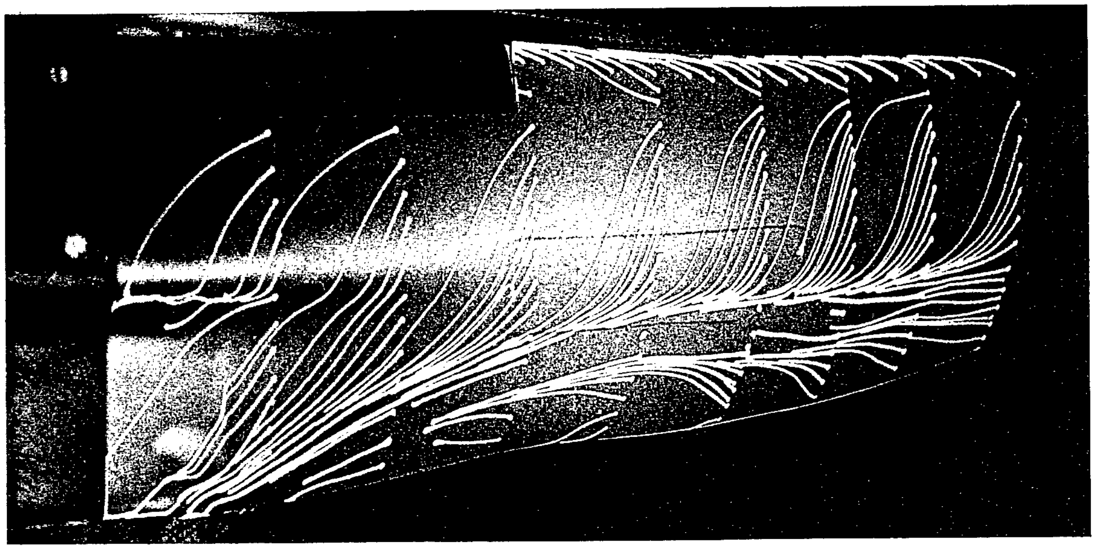

LEX fence off

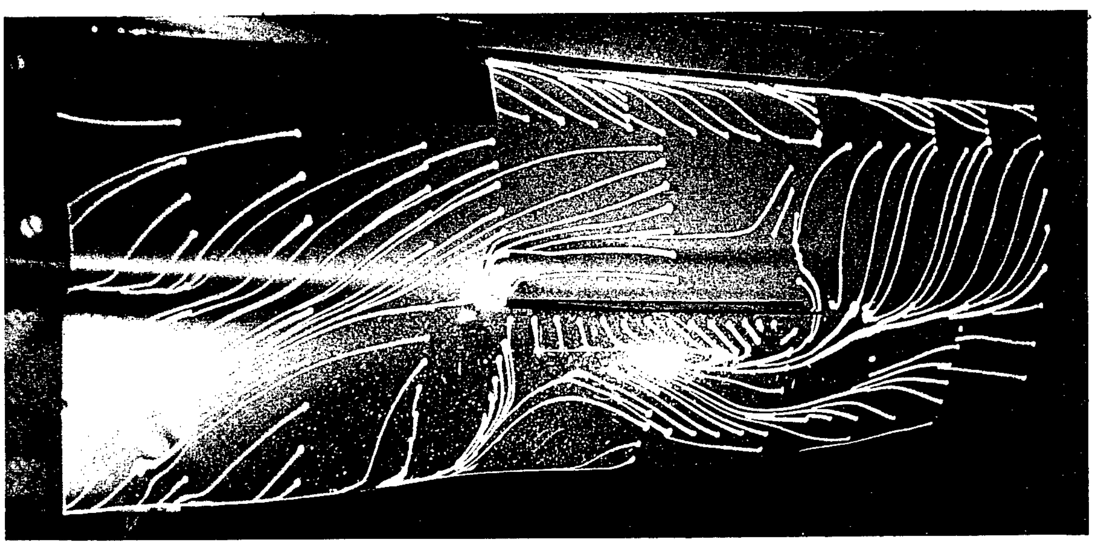

LEX fence on

Figure 14(b). Surface flow pattern near fence on LEX upper surface of wind tunnel model (Angle of attack = 25.4°; leading-edge flap deflection = 35°; trailing-edge flap deflection = 0°; velocity = 50 m/s)

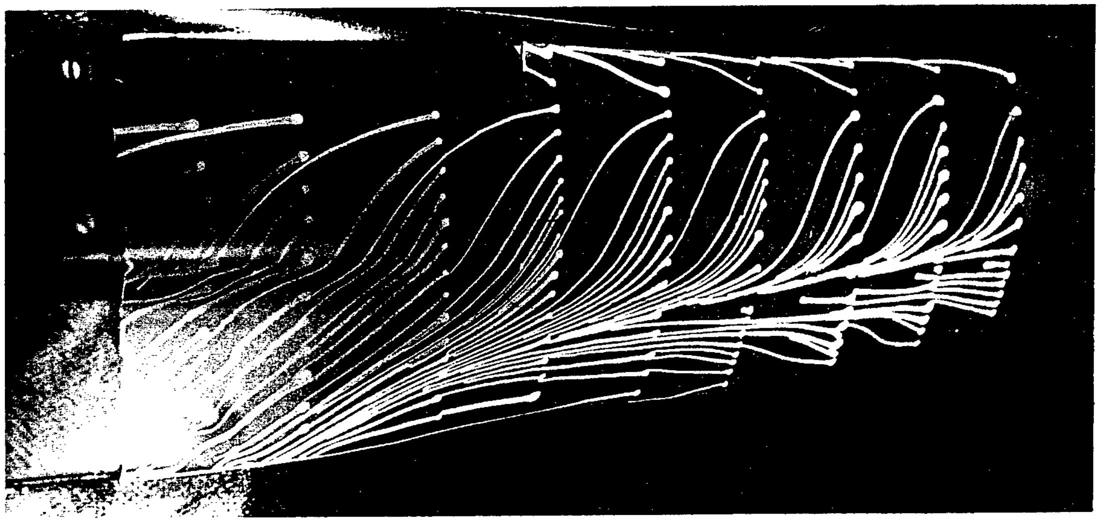

LEX fence off

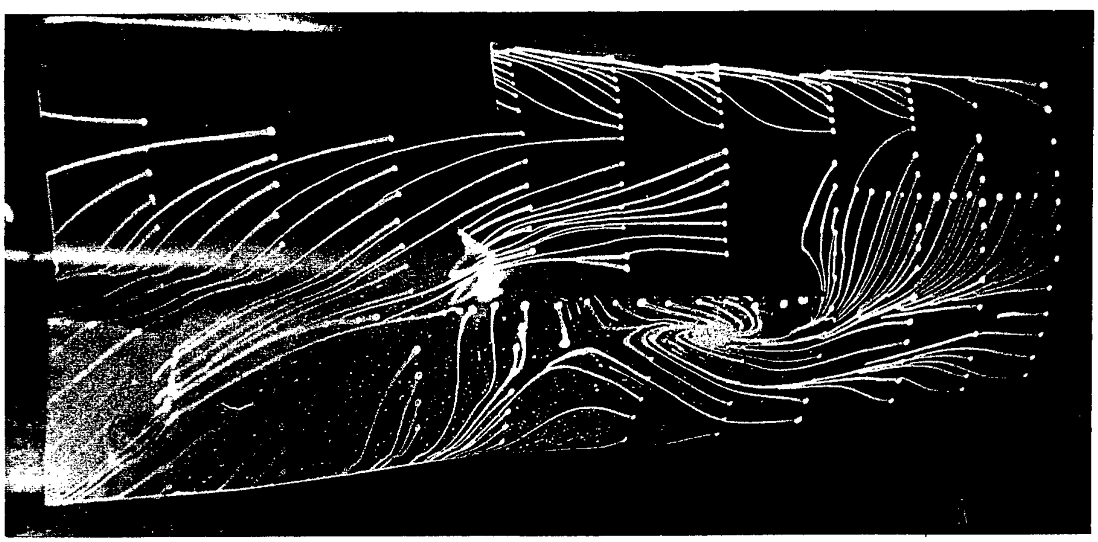

LEX fence on

Figure 14(c). Surface flow pattern near fence on LEX upper surface of wind tunnel model (Angle of attack = 30.5°; leading-edge flap deflection = 35°; trailing-edge flap deflection = 0°; velocity = 50 m/s)

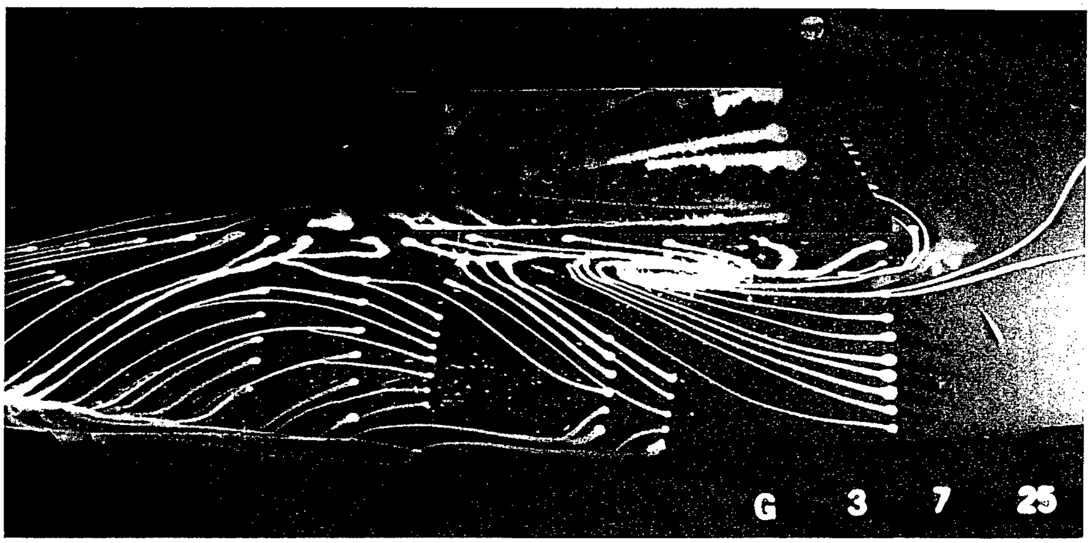

← Direction of freestream flow
Outboard side of fence

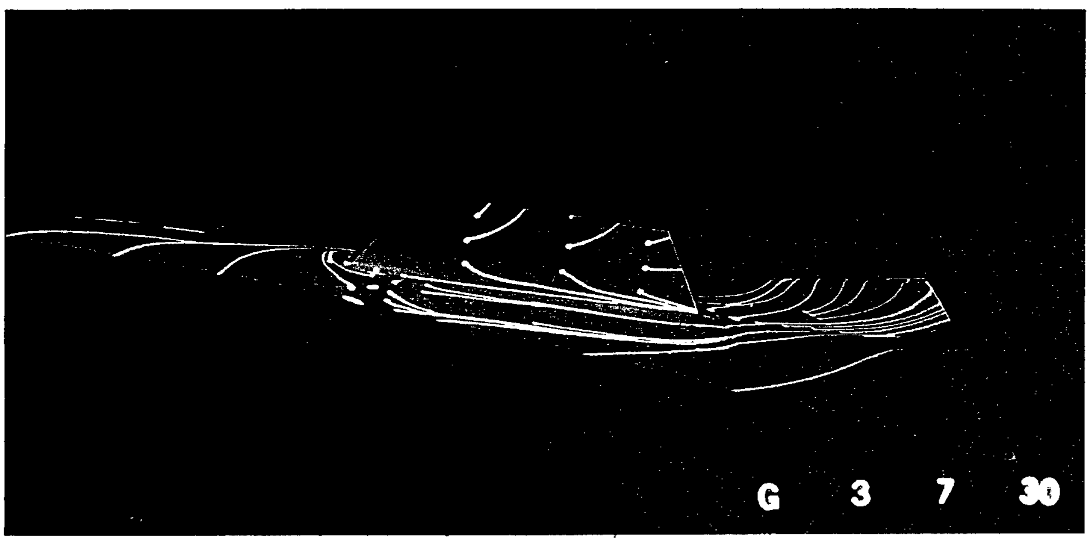

Direction of freestream flow →
Inboard side of fence

Figure 15. Surface flow pattern on fence and LEX upper surface of wind tunnel model (Angle of attack = 30.5°; leading-edge flap deflection = 35°; trailing-edge flap deflection = 0°; velocity = 50 m/s)

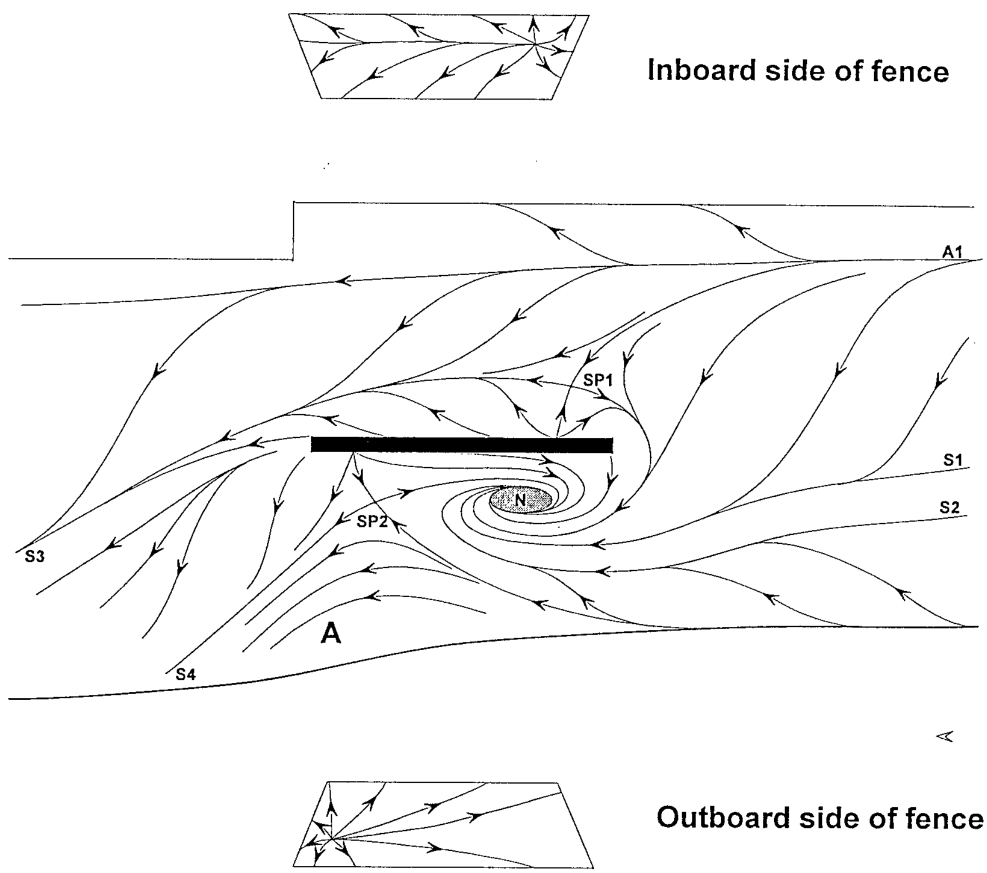

Figure 16. Postulated surface flow pattern around F/A-18 LEX fence

DISTRIBUTION LIST

Effect of the Leading Edge Extension (LEX) Fence on the Vortex Structure over the F/A-18

D. H. Thompson

AUSTRALIA

1. DEFENCE ORGANISATION

S&T Program
Chief Defence Scientist } shared copy
FAS Science Policy } shared copy
AS Science Corporate Management } shared copy
Director General Science Policy Development
Counsellor Defence Science, London (Doc Data Sheet)
Counsellor Defence Science, Washington (Doc Data Sheet)
Scientific Adviser to MRDC Thailand (Doc Data Sheet)
Director General Scientific Advisers and Trials/Scientific Adviser Policy and Command (shared copy)
Navy Scientific Adviser (3 copies Doc Data Sheet and one copy of the distribution list)
Scientific Adviser - Army (Doc Data Sheet and distribution list)
Air Force Scientific Adviser
Director Trials

Aeronautical and Maritime Research Laboratory
Director

Electronics and Surveillance Research Laboratory
Director

Air Operations Division:
Chief
Research Leader - Aircraft Performance
Head - Flight Mechanics Technology
Author: D. H. Thompson (10 copies)
B. D. Fairlie (9 copies, including 8 for distribution to TTCP HTP-5)
M. K. Glaister

Airframes and Engines Division:
C. A. Martin
D. J. Sherman
S. D. Hill
W. Waldman

DSTO Library
Library Fishermens Bend
Library Maribyrnong
Library DSTOS (2 copies)
Australian Archives
Library, MOD, Pyrmont (Doc Data Sheet)

Forces Executive
Director General Force Development (Sea) (Doc Data Sheet)
Director General Force Development (Land) (Doc Data Sheet)

Army
ABCA Office, G-1-34, Russell Offices, Canberra (4 copies)

Air Force
Aircraft Research and Development Unit

S&I Program
Defence Intelligence Organisation
Library, Defence Signals Directorate (Doc Data Sheet only)

B&M Program (libraries)
OIC TRS, Defence Regional Library, Canberra
Officer in Charge, Document Exchange Centre (DEC), 1 copy
    *US Defence Technical Information Centre, 2 copies
    *UK Defence Research Information Center, 2 copies
    *Canada Defence Scientific Information Service, 1 copy
    *NZ Defence Information Centre, 1 copy
    National Library of Australia, 1 copy

2. UNIVERSITIES AND COLLEGES

Australian Defence Force Academy
    Library
    Head of Aerospace and Mechanical Engineering
Deakin University, Serials Section (M list), Deakin University Library, Geelong, 3217
Senior Librarian, Hargrave Library, Monash University
Librarian, Flinders University
University of Melbourne, Engineering Library
University of Sydney, Engineering Library
University of New South Wales, Library
RMIT, Aerospace Engineering Department

3. OTHER ORGANISATIONS

NASA (Canberra)
AGPS

OUTSIDE AUSTRALIA

4. ABSTRACTING AND INFORMATION ORGANISATIONS

INSPEC: Acquisitions Section Institution of Electrical Engineers
Library, Chemical Abstracts Reference Service
Engineering Societies Library, US
Materials Information, Cambridge Scientific Abstracts, US
Documents Librarian, The Center for Research Libraries, US

5. INFORMATION EXCHANGE AGREEMENT PARTNERS

Acquisitions Unit, Science Reference and Information Service, UK
Library - Exchange Desk, National Institute of Standards and Technology, US

CANADA

NRC National Aeronautical Establishment
Library
Mr. B. H. K. Lee

University of Toronto, Institute for Aerospace Studies
Library

FRANCE

ONERA
Library

INDIA

National Aeronautical Laboratory
Information Centre

JAPAN

National Aerospace Laboratory
Library

NETHERLANDS

National Aerospace Laboratory (NLR)
Library

Delft University of Technology, Dept. of Aerospace Engineering
Dr. H. W. M. Hoeijmakers
Mr. N. G. Verhaagen

SWEDEN

Aeronautical Research Institute
Library

UNITED KINGDOM

Defence Research Agency
Bedford
Library
Farnborough
Library

Aircraft Research Association
Library

British Aerospace (Warton)
Library

Universities and Colleges

Bristol	Engineering Library Professor M. V. Lowson, Dept. of Aerospace Engineering
Cambridge	Engineering Library
Southampton	Library
Imperial College	Aeronautics Library
Cranfield Inst. of Technology	Library

UNITED STATES OF AMERICA

NASA Scientific and Technical Information Facility

NASA Ames Research Center
Mr. L. Meyn

NASA Langley Research Center
Mr. J. R. Chanbers
Mr. W. L Sellers
Mr. G. E. Erickson
Mr. J. E. Lamar

Eidetics International
Mr. G. N. Malcolm

Vigyan Research Associates Inc.
Dr. D. M. Rao

Universities and Colleges
University of Notre Dame, Professor R. C. Nelson, Dept. of Aerospace Engineering
Wichita State University, Professor W. H. Wentz, Institute for Aviation Research

SPARES (10 copies)

Total number of copies: 112

Page classification: UNCLASSIFIED

DEFENCE SCIENCE AND TECHNOLOGY ORGANISATION DOCUMENT CONTROL DATA						1. PRIVACY MARKING/CAVEAT (OF DOCUMENT)
2. TITLE Effect of the Leading-Edge Extension (LEX) Fence on the Vortex Structure over the F/A-18			3. SECURITY CLASSIFICATION (FOR UNCLASSIFIED REPORTS THAT ARE LIMITED RELEASE USE (L) NEXT TO DOCUMENT CLASSIFICATION) Document (U) Title (U) Abstract (U)			
4. AUTHOR(S) D. H. Thompson			5. CORPORATE AUTHOR Aeronautical and Maritime Research Laboratory PO Box 4331 Melbourne Vic 3001			
6a. DSTO NUMBER DSTO-TR-0489	6b. AR NUMBER AR-008-381		6c. TYPE OF REPORT Technical Report		7. DOCUMENT DATE February 1997	
8. FILE NUMBER M1/8/861	9. TASK NUMBER DST 95/167	10. TASK SPONSOR DST		11. NO. OF PAGES 50	12. NO. OF REFERENCES 14	
13. DOWNGRADING/DELIMITING INSTRUCTIONS			14. RELEASE AUTHORITY Chief, Air Operations Division			
15. SECONDARY RELEASE STATEMENT OF THIS DOCUMENT *Approved for public release* OVERSEAS ENQUIRIES OUTSIDE STATED LIMITATIONS SHOULD BE REFERRED THROUGH DOCUMENT EXCHANGE CENTRE, DIS NETWORK OFFICE, DEPT OF DEFENCE, CAMPBELL PARK OFFICES, CANBERRA ACT 2600						
16. DELIBERATE ANNOUNCEMENT No limitations						
17. CASUAL ANNOUNCEMENT Yes						
18. DEFTEST DESCRIPTORS F/A-18 aircraft; Vortex flows; Vortex breakdown; Flow visualisation; Water tunnel tests; Wind tunnel tests.						

19. ABSTRACT

The effects of the Leading Edge Extension (LEX) fence on the vortex structure over the F/A-18 at moderate to high angles of attack were studied using a 1/9 scale wind tunnel model and a 1/48 scale water tunnel model. Measurements at the tip of one of the vertical fins of the wind tunnel model confirmed that the fence reduced fin vibration caused by vortex breakdown. Flow visualisation in the water tunnel and in the wind tunnel showed that the fence caused the formation of a second LEX vortex, of the same sense as the main LEX vortex, but originating on the LEX leading edge outboard of the fence. Visualisation of the surface flow around the fence showed in detail how the fence caused the second LEX vortex. The effects on vortex breakdown and fin vibration of the interaction between the main and second LEX vortices are discussed.

Page classification: UNCLASSIFIED